

## Seasonal estimates of riparian evapotranspiration using remote and in situ measurements

D.C. Goodrich<sup>a,\*</sup>, R. Scott<sup>b</sup>, J. Qi<sup>c</sup>, B. Goff<sup>a</sup>, C.L. Unkrich<sup>a</sup>, M.S. Moran<sup>a</sup>,  
D. Williams<sup>b</sup>, S. Schaeffer<sup>d</sup>, K. Snyder<sup>b</sup>, R. MacNish<sup>b</sup>, T. Maddock<sup>b</sup>,  
D. Pool<sup>e</sup>, A. Chehbouni<sup>f</sup>, D.I. Cooper<sup>g</sup>, W.E. Eichinger<sup>h</sup>,  
W.J. Shuttleworth<sup>b</sup>, Y. Kerr<sup>i</sup>, R. Marsett<sup>a</sup>, W. Ni<sup>a</sup>

<sup>a</sup> USDA–ARS, Southwest Watershed Research Center, Tucson, AZ 85719, USA

<sup>b</sup> University of Arizona, Tucson, AZ, USA

<sup>c</sup> Michigan State University, East Lansing, MI, USA

<sup>d</sup> University of Arkansas, Fayetteville, AR, USA

<sup>e</sup> US Geological Survey, Water Resources Division, Tucson, AZ, USA

<sup>f</sup> IRD/IMADES, Hermosillo, Sonora, Mexico

<sup>g</sup> Las Alamos National Laboratory, Las Alamos, NM, USA

<sup>h</sup> University of Iowa, Iowa City, IA, USA

<sup>i</sup> CESBIO, Toulouse, France

### Abstract

In many semi-arid basins during extended periods when surface snowmelt or storm runoff is absent, groundwater constitutes the primary water source for human habitation, agriculture and riparian ecosystems. Utilizing regional groundwater models in the management of these water resources requires accurate estimates of basin boundary conditions. A critical groundwater boundary condition that is closely coupled to atmospheric processes and is typically known with little certainty is seasonal riparian evapotranspiration (ET). This quantity can often be a significant factor in the basin water balance in semi-arid regions yet is very difficult to estimate over a large area. Better understanding and quantification of seasonal, large-area riparian ET is a primary objective of the Semi-Arid Land-Surface-Atmosphere (SALSA) Program. To address this objective, a series of interdisciplinary experimental campaigns were conducted in 1997 in the San Pedro Basin in southeastern Arizona. The riparian system in this basin is primarily made up of three vegetation communities: mesquite (*Prosopis velutina*), sacaton grasses (*Sporobolus wrightii*), and a cottonwood (*Populus fremontii*)/willow (*Salix goodingii*) forest gallery. Micrometeorological measurement techniques were used to estimate ET from the mesquite and grasses. These techniques could not be utilized to estimate fluxes from the cottonwood/willow (C/W) forest gallery due to the height (20–30 m) and non-uniform linear nature of the forest gallery. Short-term (2–4 days) sap flux measurements were made to estimate canopy transpiration over several periods of the riparian growing season. Simultaneous remote sensing measurements were used to spatially extrapolate tree and stand measurements. Scaled C/W stand level sap flux estimates were utilized to calibrate a Penman–Monteith model to enable temporal extrapolation between synoptic measurement periods. With this model and set of measurements, seasonal riparian vegetation water use estimates for the riparian corridor were obtained. To validate these models, a 90-day pre-monsoon water balance over a 10 km section of the river was carried out. All components of the water balance, including riparian ET, were

\*Corresponding author.

independently estimated. The closure of the water balance was roughly 5% of total inflows. The ET models were then used to provide riparian ET estimates over the entire corridor for the growing season. These estimates were approximately 14% less than those obtained from the most recent groundwater model of the basin for a comparable river reach. Published by Elsevier Science B.V.

*Keywords:* Riparian evapotranspiration; Penman–Monteith model; Cottonwood/willow transpiration; SALSA Program; Interdisciplinary; Water balance

## 1. Introduction

In many semi-arid basins, groundwater resources sustain human habitation, agriculture and riparian ecosystems. Utilizing regional groundwater models to aid in water resources management requires accurate estimates of basin boundary conditions. A critical groundwater boundary condition that is closely coupled to atmospheric processes and is poorly quantified is the seasonal riparian evapotranspiration (ET) (Maddock et al., 1998).

Improved estimates of riparian ET derived from groundwater and its seasonal distribution are necessary to improve regional groundwater models so that they can be used more reliably as near-term management tools versus their typical use for long-range planning. Typical groundwater modeling studies are done at an annual time scale. This ignores the seasonal variations inherent in the normal growing cycle and periods of runoff (Maddock et al., 1998). With a better understanding of the riparian ET processes, we intend to develop a better groundwater model ET module based on potential functions that can be directly coupled to similar potential-based flux functions for aquifer and streamflow. This will alleviate the problems noted in Maddock et al. (1998) of the inconsistent treatment of ET processes related to precipitation and runoff versus those originating from groundwater.

To properly couple riparian ET with groundwater models, it is also critical to identify plant water sources (groundwater, surface runoff, precipitation, or vadose zone). In many cases, water from multiple sources are used by the plants. The mixture of the plant water sources may also vary seasonally with surface water availability and the depth to groundwater (Snyder and Williams, 2000). Another difficulty in estimating riparian ET in semi-arid rivers is the complicated geometry of a typical riparian corridor forest gallery. These corridor forest galleries are often relatively high (~5–20 m), narrow (~20–200 m), long, and sin-

uous, as they typically follow the alluvial floodplain. This geometry precludes the use of classical micrometeorological flux measurements (e.g. Bowen ratio, eddy covariance) as the required fetch conditions are not satisfied (see Hipps et al., 1998 for further detail).

Overcoming these difficulties to provide a better understanding and quantification of large-area riparian ET is one of the primary objectives of the SALSA Program (see overview by Goodrich et al., 2000). To address this objective, a number of integrated interdisciplinary experimental field campaigns were conducted in the Upper San Pedro Basin (USPB) riparian corridor in southeastern Arizona during 1997. Isotopic and plant physiology measurements were carried out to identify plant water sources over a range of hydrologic regimes. A scanning Raman LIDAR (Light Detection And Ranging) laser system was deployed (Cooper et al., 2000; Eichinger et al., 2000) and sap flux measurements were made (Schaeffer et al., 2000) to estimate C/W ET. Simultaneous high-resolution remote sensing images were also acquired to remotely estimate ET. None of these measurements provide ET estimates over the entire growing season for the entire riparian corridor. However, our intent in this paper is to utilize combinations of these measurements and methods with a stepwise scaling approach, and a calibrated Penman–Monteith model to address the following primary objectives.

1. Scale riparian ET estimates whose water source is derived from groundwater both spatially and temporally over the entire growing season and the entire riparian corridor.
2. Assess the validity of the scaling relationships by carrying out a water balance on a portion of the riparian system during a pre-monsoon period.

The presentation is organized as follows. Section 2 contains background information and an overview of prior methods used to estimate riparian ET. Section 3, on materials and methods, contains the experimental site description as well as a description of

the ground and remote sensing measurements. Section 4 describes the theory and modeling approach to scale in situ measurements as well as the water balance used to assess the validity of the scaling and modeling approach. Results are presented and discussed in Section 5. A brief summary is contained in Section 6. This is followed by conclusions and recommendations contained in Section 7.

## 2. Background

The direct and indirect influence of riparian ET on basin surface and groundwater resources has been noted in numerous prior studies (Croft, 1948; Lines, 1996; Bowie and Kam, 1968; Federer, 1973; Singh, 1968; Culler et al., 1982). Both Bowie and Kam (1968) and Federer (1973) noted significant impacts on streamflow by ET which were further confirmed by examination of streamflows after herbiciding or eliminating riparian vegetation (Culler et al., 1982). A variety of prior methods have utilized these observed impacts on adjacent surface water and groundwater to indirectly estimate riparian ET.

Early methods analyzed baseflow recession curves at various times of the year to estimate riparian ET at monthly and seasonal time scales (Langbein, 1942; Riggs, 1953; Whelan, 1950; Hall, 1968). On a shorter time scale Tschinkel (1963) and Reigner (1966) utilize diurnal hydrograph changes to compute daily riparian ET. Daniel (1976), in a similar manner to Tschinkel (1963), presents a method to compute ET over several months based on the difference between observed streamflow and the theoretical “potential streamflow” determined from a recession index. Lines (1996) utilized this approach to estimate riparian ET on the Mojave River for selected years in which surface runoff was minimal by integrating the estimated streamflow depletion throughout the riparian growing season. Corell et al. (1996) and Goodrich et al. (1998) carried out a similar analysis for the San Pedro River in southeastern Arizona. While periods without ET and runoff recharge can typically be found by examining various periods of the discharge record, the requirement for absence of pumping in this approach is typically more restrictive in any developed basin. When storm runoff does occur, the method also assumes baseflows can be easily separated from storm

runoff. As noted by Maddock et al. (1998), this is not a simple task. Another difficulty with this method is determining the areal extent over which the riparian ET affects streamflow. If a reach becomes intermittent, this type of analysis is not applicable even though substantial riparian vegetation may be present.

Gatewood et al. (1950) provide a good description of six methods other than hydrograph analysis that were employed to estimate riparian water use in the Lower Safford Valley in Arizona. The six methods were: (1) tank or lysimeter, (2) transpiration-well, (3) seepage run, (4) water balance (inflow–outflow), (5) chloride-increase, and (6) slope-seepage. All of these methods estimate riparian ET indirectly through its observed effects on related stream or aquifer characteristics. As in the case of integrating streamflow depletion, the transpiration-well, chloride-increase, and slope-seepage methods all exhibit the same difficulties of estimating the areal extent of riparian vegetation responsible for the indirectly determined riparian water use. In a well-controlled tank or lysimeter, accurate ET estimates can be obtained via a water balance calculation but scaling-up these measurements to the riparian corridor level has been problematic. Lines (1996) noted that lysimeter or tank ET measurements (e.g. Gatewood et al., 1950; van Hylckama, 1980) did not agree well with annual ET estimates derived from streamflow depletion along the Mojave River. Weeks et al. (1987) noted that the high rates measured by lysimeters or tanks are likely due to oasis and plant age effects and are likely to represent maximum ET rates occurring in a non-water limited situation. The seepage run method can only be applied in reaches with perennial flow and with flows large enough to be accurately measured by current meter methods. Both of these conditions are violated in the San Pedro Basin as well as numerous semi-arid riparian systems.

Other meteorologically based methods such as the often employed Blaney–Criddle (Shuttleworth, 1993) approach have also been employed to estimate riparian ET. In this empirical, temperature-based method, ET rates are scaled by vegetation area to derive monthly ET estimates. However, temperature-based ET-estimation methods are not recommended unless this is the only available data source (Shuttleworth, 1993). Shuttleworth (1993) also notes that while the complexity of the Blaney–Criddle equation “is a tribute to the loyalty of its proponents, it precludes

ready interpretation in terms of a physically realistic equivalent”.

More recently, several additional methods have been employed to estimate riparian ET. Gay and Fritschen (1979) and Weeks et al. (1987) employed micrometeorological and energy balance techniques to estimate ET from large, dense salt cedar riparian stands. Unland et al. (1998) employed similar techniques over a dense mesquite bosque located in the Santa Cruz riparian system. Comparable methods were used in this study to measure ET over relatively large uniform stands of mesquite and sacaton grasses (Scott et al., 2000). However, as noted in Section 1, the necessary fetch conditions for these techniques are typically not met in semi-arid riparian forest galleries.

### 3. Experiment and measurements

#### 3.1. Site description

The USPB, located in the semi-arid borderland of southeastern Arizona and northeastern Sonora, is

a broad, high-desert valley bordered by mountain ranges and bisected by a narrow riparian corridor (Fig. 1). The vibrant San Pedro riparian ecosystem is primarily made up of three vegetation communities dominated by mesquite, grasses, and C/W forests. Portions of the river contain some of the healthiest desert riparian ecosystems remaining in the southwestern US (Grantham, 1996; Stromberg, 1998). This riparian forest supports a great diversity of species — some endangered with extinction — and is widely recognized as a regionally and globally important ecosystem (World Rivers Review, 1997; Kingsolver, 2000). In 1988, the United States Congress established the San Pedro Riparian National Conservation Area (SPRNCA), the first of its kind in the nation, to protect riparian resources along 60 km of river north of the US–Mexico border.

However, there is serious concern that nearby groundwater withdrawals have affected the quantity and timing of groundwater reaching the San Pedro River (Pool and Coes, 1999) as groundwater sustains perennial flow in large reaches of the river (Richter and Richter, 1992; CEC, 1999). The close coupling

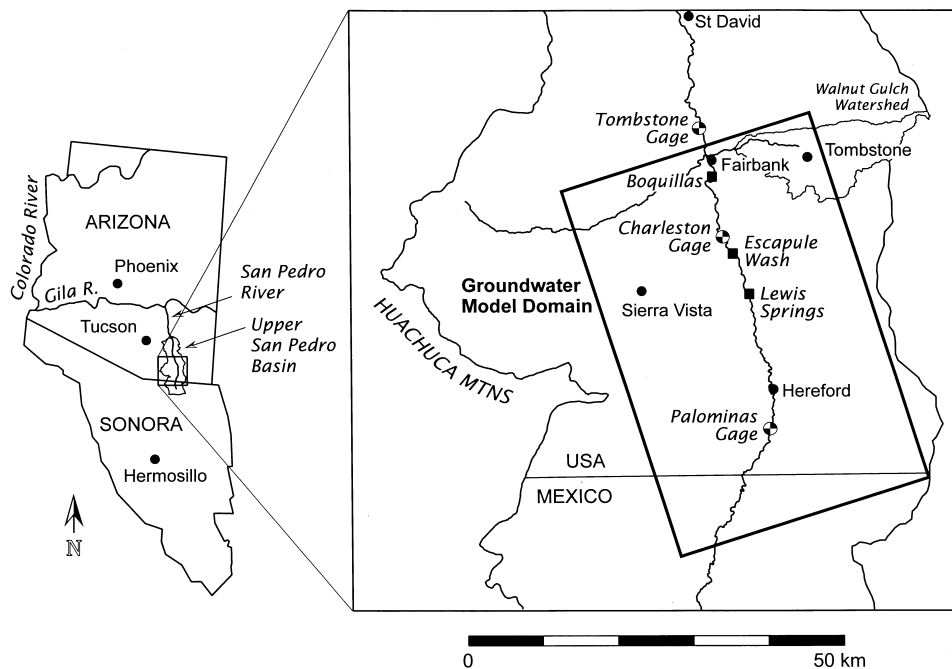


Fig. 1. Location of the San Pedro River Basin and pertinent geographic and measurement locations. The box corresponds to the boundaries of the groundwater model of Corell et al. (1996).

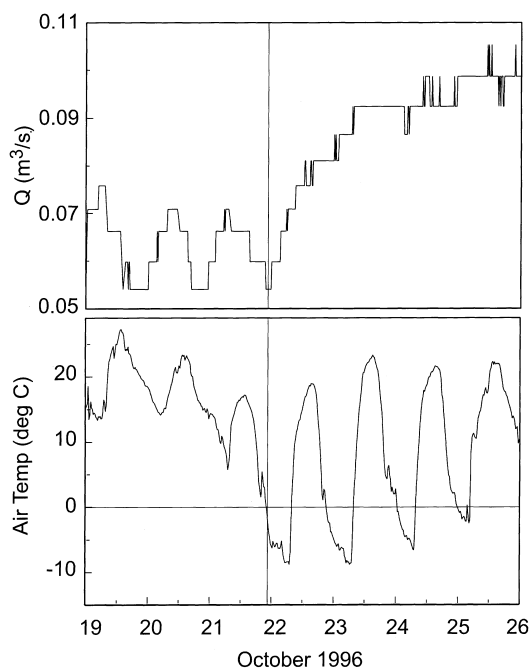


Fig. 2. San Pedro River discharge from the USGS gage at Charleston, AZ (top); air temperature measured at mesquite tower, Lewis Springs, AZ (bottom).

between riparian ET and streamflows in the USPB is indirectly illustrated in Fig. 2. In the top portion of this figure, discharge from the US Geological Survey (USGS) stream gage at Charleston (Fig. 1) is plotted from 19 to 26 October 1996. The bottom part of the figure illustrates air temperature from the Lewis Springs site (Fig. 1) south of the Charleston Gage. Prior to the first hard freeze, occurring late on 21 October 1996 the streamflow exhibits a distinct diurnal pattern that is closely correlated with air temperature and presumably riparian ET. After the freeze, the diurnal pattern immediately dissipates and the discharge increases indicating the hard freeze put a halt to riparian ET. Similar diurnal patterns in shallow well water levels in the floodplain alluvium during the riparian growing season illustrate the close coupling between groundwater, surface water, riparian vegetation, and atmospheric processes in the USPB (MacNish et al., 1998). Current estimates of riparian ET water use are substantial in this basin. Based on calibrated groundwater model estimates (Vionnet and Maddock, 1992; Corell et al., 1996), riparian ET accounts for

roughly 40% of the total basin groundwater discharge. Therefore, better understanding and methods to quantify riparian ET are essential to the management and preservation of this system.

The most intensive set of coordinated measurements took place in the perennial river reach surrounding the Lewis Springs site. Different hydrologic regimes were included in the study by making a subset of measurements at the intermittent Boquillas Ranch site and the ephemeral Escapule wash site (Fig. 1). Measurements were made prior to and throughout the 1997 riparian growing season. While some measurements were made on a near-continuous basis (e.g. meteorology, stream stage), five intensive synoptic measurement sets were made over periods ranging in length from 48 to 120 h. The synoptic measurement periods spanned a period from March to October during the following days of the year (DOY — Julian Day Of Year) 111–112, 158–160, 191–194, 223–228, and 285–289. This period spans the pre-green-up and growing season to allow for characterization of the seasonal variations in ET, and surface-water-groundwater interactions. During these synoptic measurement periods, a variety of coordinated remotely sensed and ground measurements were made.

### 3.2. Remotely sensed measurements

An essential component in estimating riparian ET is the determination of the area for various vegetation types or classes within the riparian corridor. The primary data sources utilized for the riparian vegetation classification were: (1) a 12-band thematic mapper simulator (TMS) deployed aboard a NASA Jet Propulsion Laboratory aircraft, and (2) high-resolution color infrared (CIR) photography obtained from a 9 in. format mapping camera aboard a USDA-ARS aircraft from Weslaco, TX (Moran et al., 1998; Goodrich et al., 2000). The riparian corridor was defined using a combination of USGS one-arc second digital elevation model (DEM) data and CIR photography. A detailed discussion of the procedures and imagery employed to obtain the vegetation classification and the respective class areas is presented in Appendix A.

Single-channel thermal data from an Inframetrics sensor (inclusion of company or product names is for information purposes only and does not indicate

endorsement) were also acquired over a section of the riparian corridor from approximately Hereford to Fairbank in 1997 during four of the synoptic measurement periods (21 April, 13 July, 12 August, 14 October, corresponding to DOY 111, 194, 224, and 287, respectively).

To aid in estimation of seasonal riparian ET over the entire corridor, the single-channel thermal remotely sensed data were examined to assess whether they could be used to discern stream reaches with differentially stressed riparian vegetation due to significant hydrologic changes from image to image. For example, during the April overflight (DOY 111), the entire reach from Lewis Springs to Fairbank had surface water present in the channel. During the July overflight (DOY 194), reaches roughly 6 km downstream of the Charleston USGS gage dried up. In this area, the cottonwood trees were observed to be dropping leaves and yellowing, presumably from water stress. By the time of the August overflight (DOY 224), monsoon floods had inundated the entire San Pedro River reach under study.

### 3.3. Ground measurements

Three primary vegetation communities in the San Pedro riparian corridor are capable of utilizing significant quantities of groundwater including the cottonwood/willow (C/W) forest gallery, mesquite, and phreatophytic sacaton grasslands. An initial objective is to estimate the amount of riparian ET originating from groundwater for each of these groups on a per unit area of vegetation basis. To address this objective, a variety of ground-based measurements were made. These measurements are described in more detail in the preface (Goodrich et al., 2000) as well as in a number of the other papers in this issue. Measurements used to directly address the objectives of this study are briefly described herein. Other measurements are noted with appropriate references.

The majority of ground-based measurements were made at the Lewis Springs site. Continuous measurements of water levels in a transect of six deep wells, meteorology and fluxes (Bowen ratio) over the riparian grass and mesquite thicket (Scott et al., 2000), and stream stage were made during all of 1997. Measurements taken during the synoptic runs included hourly

stream stage and water levels from five river sections and the piezometer network within the Lewis Springs reach, stream discharge measurements determined by current metering, dye-dilution, and an in-stream flume for the June campaign (see summary by Maddock et al., 1998). A continuous stage recorder was maintained by the USGS at cross-section three near Lewis Springs. Throughout 1997, a series of 18 current meter discharge measurements were made at this location to establish a stage–discharge relationship for low flows. Tree sap flow, water potential, stomatal conductance, and water sources using stable isotopes were determined for cottonwood and willow during each of the synoptic campaigns to capture variations in transpiration demand as a function of atmospheric demand and water availability (Schaeffer et al., 2000). The sap flux measurements were made on a small sample of trees at the perennial Lewis Springs and ephemeral Escapule Wash site. We were not able to measure ET from the understory of the C/W forest gallery with this data collection methodology.

Water sources using stable oxygen and hydrogen isotope ratios were determined for mesquite, cottonwood, willow and several other species at Lewis Springs site as well as an intermittent and ephemeral riparian stream reach (at Boquillas and Escapule locations, respectively — see Fig. 1). These data allowed the proportion and magnitude of surface water use by the gallery trees as a function of groundwater availability to be evaluated (Snyder and Williams, 2000). During aircraft overflights, ground-based remotely sensed data as well as an array of vegetation characteristics were collected for calibration purposes (Moran et al., 2000).

During the August campaign, additional instrumentation was deployed at the Lewis Springs site from 8 to 19 August. This included an array of eddy correlation flux instrumentation (see ET summary by Hips et al., 1998), a scintillometer, and the Las Alamos National Laboratory Raman LIDAR system (Cooper et al., 2000). During the first portion of the August campaign, the LIDAR was deployed on the east bank of the San Pedro River at Lewis Springs. After several days, the LIDAR was moved to the west bank and the flux instruments were redeployed across the highly heterogeneous vegetation types under the path of the scintillometer.

## 4. Theory and approach

The riparian ET experiments were designed to obtain representative measurements at the Lewis Springs site over the primary vegetation types and spatially scale these measurements using remotely sensed data over a larger portion of the corridor. Temporal scaling (or extrapolation) between synoptic measurement periods was to be obtained either from continuous ET measurements over the various vegetation types or from a meteorologically driven model. The following approaches will be presented: (1) a methodology for scaling the ET estimates in time and space; (2) a modeling approach to temporally scale (extrapolate) the C/W transpiration estimates; (3) a water balance over a 10 km reach of the riparian corridor to check the riparian ET estimates.

### 4.1. Scaling approach

The scaling approach used was dependent both on the type of riparian vegetation and the measurement method employed. Continuous measurements of the local meteorology and several of the energy balance components were made through the growing season over relatively uniform areas of the sacaton grass and mesquite. The Bowen ratio technique was used with these data used to estimate ET [ $\text{LT}^{-1}$ ] in for these vegetation types (Scott et al., 2000). The remotely sensed estimates of sacaton and mesquite area were then used to scale these measurements spatially over portions of the riparian corridor to obtain ET as a volume per unit time. Because continuous measurements were available, these estimates could simply be integrated over the desired time period to obtain a volume of ET from mesquite and sacaton for the overall water balance.

Scaling the C/W transpiration estimates obtained from sap flux measurements presented additional challenges. With tree coring, the basic data collected consisted of sap flux (tree transpiration), expressed on a per unit sapwood area basis per unit time ( $\text{g H}_2\text{O cm}^{-2} \text{h}^{-1}$ ). The first step to scale individual tree estimates of transpiration to patch and stand estimates involved relating sapwood area to an easily measured parameter. In this case, basal tree diameter was related to sapwood area by a separate regression analysis for C/W trees (Schaeffer et al., 2000). In the next phase of scaling, 12 C/W forest patches

(five newly established and seven successional advanced) were selected based on ease of identification on the remotely sensed imagery and high-resolution CIR photography (see Fig. 1, Schaeffer et al., 2000). A number of the patches were also selected as they were within the LIDAR data acquisition area (Cooper et al., 2000). The areal canopy area of each of the patches was measured using the aerial imagery. The basal diameters of all trees in each patch were then measured, as well as the leaf area index using a light extinction meter.

The next step in scaling the sap flux measurements was from the patch level to a spatially continuous C/W stand on a river reach roughly one-half km long at the Lewis Springs site. By scaling to the level of a larger river reach, a more representative sample of trees was obtained and the uncertainty in patch area definition was reduced. Canopy area definition from outlining the perimeter of smaller patches on digital imagery is made difficult by their irregular shape and effects from shadowing. To overcome this problem and provide stand level transpiration estimates, breast height diameters of all C/W trees were measured in a roughly 600 m stream reach at Lewis Springs (2238 trees) and a roughly 1150 m stream reach at the Escapule site (256 trees). By including larger continuous stands of C/W, the perimeter to area ratio of the canopy and presumably the uncertainty in defining the canopy area was reduced.

With these data, stand level C/W transpiration estimates were obtained continuously for each synoptic measurement period (SMP) during the times the heat pulse velocity sensors were installed in the trees. These estimates were obtained by first computing an average sap flux per unit sapwood area for each tree with installed sensors. The average sap flux per unit sapwood area times the sapwood area of all 2238 trees in the 600 m reach provided the volume of stand level sap flux for 30 min averages during each synoptic measurement period. This volume of sap flux as a function of time is divided by the remotely derived area of the C/W canopy to provide a C/W transpiration flux in units of [ $\text{LT}^{-1}$ ]. During the periods of sap flux measurements, this quantity can be spatially scaled further by multiplying it by the remotely estimated canopy area over any specified river reach. This does not solve the problem of temporal scaling or extrapolation of the measurements between the synoptic

measurement periods. Due to limited availability of heat pulse velocity probes, sap flux measurements were not continuously made for the entire growing season. The measurements alternated between the perennial Lewis Springs site and the ephemeral Escapule site (Schaeffer et al., 2000). To estimate C/W transpiration between, and outside the synoptic measurement periods, a model driven by more easily measured continuous variables is required.

#### 4.2. Penman–Monteith (P–M) model for C/W transpiration

The well-known P–M model (Monteith and Unsworth, 1990) was selected to model C/W transpiration throughout the riparian growing season. The P–M equation for evaporation is given by

$$\lambda_E = \frac{\Delta A + \rho_a c_p D / r_a}{\Delta + \gamma (1 + r_c / r_a)} \quad (1)$$

where  $\lambda_E$  is the evaporation ( $\text{W m}^{-2}$ ),  $\Delta$  the slope of the saturation vapor pressure/temperature curve ( $\text{kPa}^\circ\text{C}^{-1}$ ),  $A$  the available energy ( $\text{W m}^{-2}$ ),  $\rho_a$  the density of moist air ( $\text{kg m}^{-3}$ ),  $c_p = 1013 \text{ J kg}^{-1} \text{ }^\circ\text{C}^{-1}$  the specific heat capacity of dry air under constant pressure,  $D$  the vapor pressure deficit (kPa),  $r_a$  the aerodynamic resistance ( $\text{s m}^{-1}$ ),  $\gamma$  the psychrometric constant ( $\text{kPa}^\circ\text{C}^{-1}$ ), and  $r_c$  the bulk canopy resistance ( $\text{s m}^{-1}$ ). In the above equation,  $\Delta$ ,  $\rho_a$ ,  $D$ , and  $\gamma$  can be approximated by formulae described by Shuttleworth (1993), based on measurements of air temperature,  $T_a$  ( $^\circ\text{C}$ ), relative humidity, RH (%), and atmospheric pressure,  $P$  (kPa). These quantities were measured at the nearby mesquite site (Scott et al., 2000), and were found to reasonably approximate conditions inside the C/W canopy. This assessment was based on comparisons to a limited set of measurements made from a 12.5 m tower inside the C/W canopy. Measurements from this tower were available in 1997 from DOY 190 to 290. For this period of time, the root mean square error (RMSE) and  $R^2$  between the vapor pressure deficit computed from measurements at the C/W tower and the mesquite tower were 0.26 kPa and 0.96, respectively. For air temperature, the RMSE was  $1.21^\circ\text{C}$ , with  $R^2 = 0.97$  between the two towers.

The available energy to the canopy is given by

$$A = S \downarrow (1 - \alpha) + L_{\text{net}} - S_t \quad (2)$$

where  $S \downarrow$  is the incoming solar radiation ( $\text{W m}^{-2}$ ),  $\alpha$  the canopy albedo,  $L_{\text{net}}$  the net long-wave radiation ( $\text{W m}^{-2}$ ), and  $S_t$  the temporary storage of energy into the tree itself (trunk and limbs) and the energy used in the photosynthesis process ( $\text{W m}^{-2}$ ). Because the bulk of the canopy is typically 10–20 m above the ground, soil heat flux contributions to the available energy for the canopy were considered negligible. The incoming solar radiation was measured over the mesquite site. Canopy albedo was estimated to be 0.18, a value which has been measured over broadleaf oak trees (Bras, 1990).  $S_t$  was estimated to be 5% of the incoming solar radiation based on work by Moore and Fisch (1986) who found that  $S_t$  ranged between 0 and 10% of the net radiation available to a tropical forest. The net long-wave radiation contribution to the available energy was calculated from a formula provided by Shuttleworth (1993, p. 4.7). Because the P–M model only applies to tree transpiration, the net radiation was adjusted to account for the portion not intercepted by the leaves using a simple Beer's law relationship from Shuttleworth and Gurney (1990). This adjustment reduced the net radiation available to the canopy by 25%.

The aerodynamic resistance ( $r_a$ ) was assumed to be the sum of the turbulent resistance between the canopy and the atmosphere from turbulent eddies and the boundary layer resistance (Thom, 1975). Due to the relatively open nature of the cottonwood canopy, the turbulent canopy resistance is assumed negligible in comparison to the boundary layer resistance. Thus  $r_a$  is assumed to equal the boundary layer resistance ( $r_b$ ). To estimate the boundary layer resistance, the model proposed by Choudhury and Monteith (1988) was used:

$$r_b = \frac{1}{Lb} \frac{\alpha_{\text{att}}}{(1 - \exp(-\frac{1}{2}\alpha_{\text{att}}))} \sqrt{\frac{w}{U}} \quad (3)$$

In this equation,  $L$  is the canopy projected leaf area index estimated to be 2.0 (Schaeffer et al., 2000). The quantity  $b$  was set equal to  $0.0067 \text{ m s}^{-1/2}$ . It is a scaling coefficient for leaf boundary layer resistance (Magnani et al., 1998).  $\alpha_{\text{att}}$  is an attenuation coefficient for wind speed inside the canopy,  $w = 0.05 \text{ m}$  is a typical leaf width, and  $U$  the wind speed outside the canopy (measured at 10 m above the ground at the mesquite site). The value for the wind attenuation

coefficient,  $\alpha_{\text{att}}$ , was set equal to 3 following Magnani et al. (1998).

The only remaining quantity required to compute C/W transpiration using Eq. (1) is the bulk canopy resistance ( $r_c$ ). This is the resistance to water vapor transport from inside the leaf to the leaf surface, which is regulated by the plant's stoma in response to environmental conditions. The canopy resistance is related to individual leaf stomatal resistance ( $r_s$ ) by the following expression (for amphistomatous leaves):

$$r_c = \frac{r_s}{2\text{LAI}} \quad (4)$$

During 1997 measurements of  $r_s$ , using a leaf porometer, were made of leaves on several trees during the April, June and August synoptic measurement periods. Personnel and economic constraints prohibited obtaining a sufficient number of leaf level stomatal resistance measurements to obtain a representative sample to approximate the required bulk canopy resistance at the tree or stand level. Therefore, the bulk canopy resistance was treated as a calibration parameter.

#### 4.2.1. Calibrating the P–M model

For each synoptic measurement period, the stand level C/W transpiration [ $\text{LT}^{-1}$ ] (2238 trees) in the Lewis Springs intensive study reach was derived by dividing the transpiration in volume per unit time by the remotely sensed estimate of the stand canopy area. Using this data, the bulk canopy resistance can be computed by using a re-arranged form of Eq. (1):

$$r_c = r_a \left[ \frac{\Delta A + \rho_a c_p D / r_a}{\gamma \lambda_E} - \frac{\Delta}{\gamma} - 1 \right] \quad (5)$$

An average bulk canopy resistance was calculated for each SMP measurement period by taking the average of all computed resistances between 09:30 and 14:30 LST under mainly sunny conditions (when the solar radiation was equal or greater than  $300 \text{ W m}^{-2}$ ).

#### 4.3. Riparian corridor water balance

As noted in Section 1, water balance methods have been utilized in the past to estimate riparian ET indirectly by attempting to measure or estimate all components of the water balance except ET and then computing ET as the residual. In this study, the inde-

pendently derived estimates of riparian ET described above are combined with independent estimates of the additional water balance components over a selected reach of the San Pedro riparian corridor for a selected period of time. If all the components of the balance are correctly measured or estimated, the residual of the water balance equation will sum to zero. Assuming there are no significant compensating errors in the water balance components, the closure of the water balance provides a check on the postulated description of water fluxes into and out of the riparian system including the methods to estimate riparian ET described above.

For our purposes, the water balance was expressed in volumetric terms ( $\text{m}^3$ ) for a specific time period and control volume as schematically illustrated in lower portion of Fig. 3 as

$$Q_{\text{in}} + \text{GW}_{\text{net}} + \text{Ppt}_{\text{ws}} - Q_{\text{out}} - T_{\text{C/W}} - \text{ET}_{\text{m}} - \text{ET}_{\text{s}} - E_{\text{ws}} - \Delta\text{Storage} = \varepsilon \quad (6)$$

The first three terms in this equation constitute water inputs into the control volume and the following five terms make up the outputs. For the inflow terms,  $Q_{\text{in}}$  is the volume of water flowing into the control volume as streamflow,  $\text{GW}_{\text{net}}$  the net volume of groundwater flowing into the control volume, and  $\text{Ppt}_{\text{ws}}$  the volume of water falling as precipitation on the stream water surface. For the outflow terms,  $Q_{\text{out}}$  is the volume of water flowing out of the control volume as streamflow,  $T_{\text{C/W}}$  the volume of water transpired by the C/W forest,  $\text{ET}_{\text{m}}$  the volume of water evaporated and transpired by the mesquite,  $\text{ET}_{\text{s}}$  the volume of water evaporated and transpired by the sacaton, and  $E_{\text{ws}}$  the volume of water evaporating from the stream water surface.  $\Delta\text{Storage}$  is the change in storage of water in the floodplain aquifer and the change in soil moisture in the unsaturated zone within the control volume, and  $\varepsilon$  the residual error of the water balance.

The water balance was performed at both the stand level and a significantly larger reach of the river. Two primary factors were considered in selecting the river reach and periods of time over which to compute the water balance. First, an attempt was made to make optimal use of the measurements in hand. Second, we attempted to minimize the impacts of our lack of knowledge of how the mesquites and C/W utilize rainfall and surface runoff (Snyder and Williams,

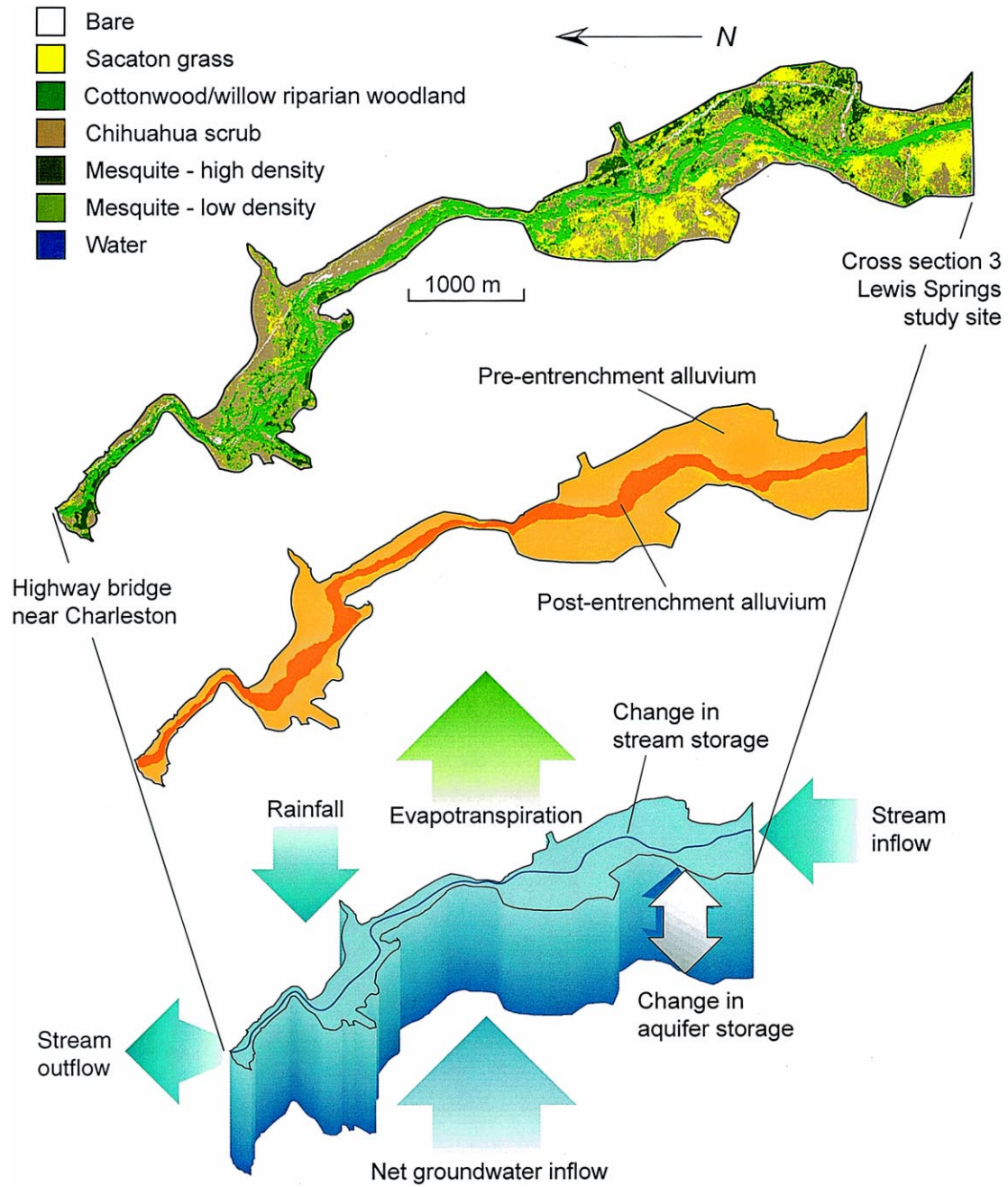


Fig. 3. Riparian corridor for the stream reach from Lewis Springs cross-section 3 to the Charleston, USGS stream gage. (Top) cover classes; (middle) pre- and post-river entrenchment alluvium boundaries; (bottom) primary water balance components for the reach.

2000). At the stand level, MacNish et al. (2000) carried out a water balance on a 122 m portion of the Lewis Springs stream reach during the March (no transpiration), April and June synoptic measurement periods. In this stream reach there were few mesquite. These measurement periods did not have any precipitation, surface runoff, or large changes in residual soil moisture over the short period of the synoptic measurement periods insuring the C/W were almost exclusively using groundwater and/or soil moisture. Also, by limiting the stand level water balance to these synoptic measurement periods we were able to assess

the validity of the scaled C/W transpiration estimates directly without the use of the calibrated P–M model.

For the water balance at the larger riparian corridor level, a 10 km river reach starting from cross-section three at the Lewis Springs study site to the USGS stream gage near Charleston, AZ was selected. An illustration of the classified land cover as well as the pre- and post-entrenchment alluvial areas for the riparian corridor for this river reach are illustrated in Fig. 3. The discharge records at the upstream (Lewis Springs) and downstream (Charleston) end of the reach (top of Fig. 4) were examined to select a time interval over

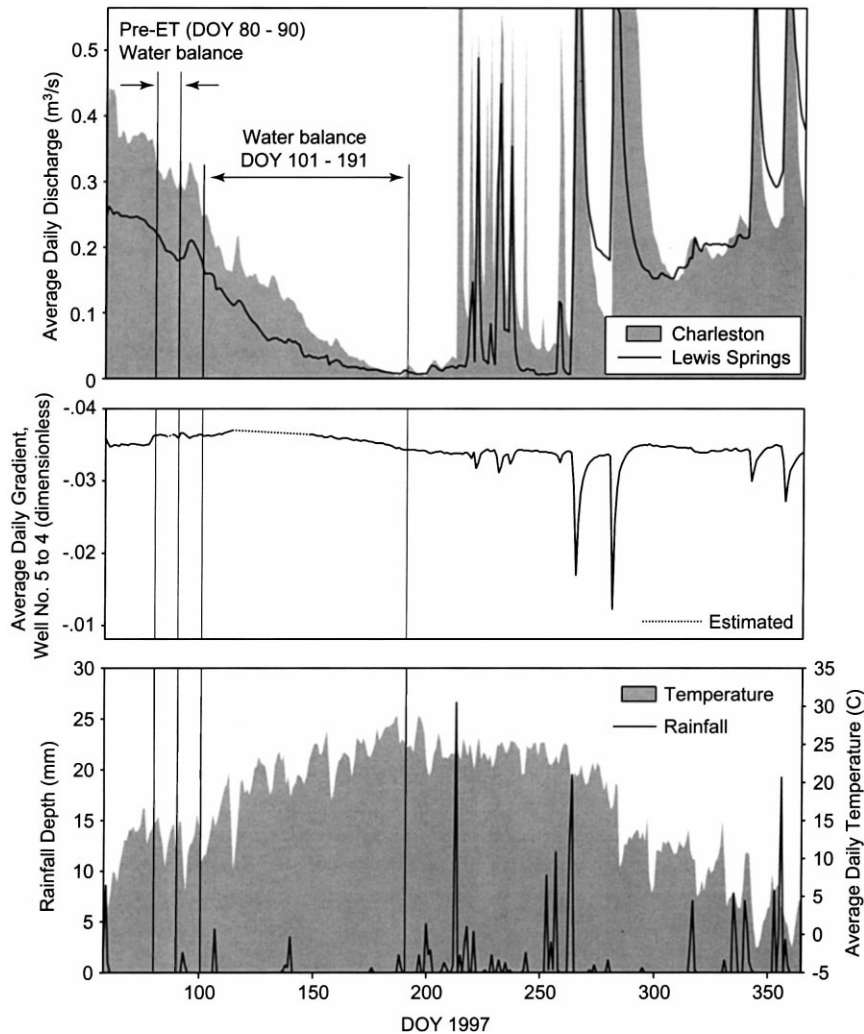


Fig. 4. (Top) streamflow at Lewis Springs cross-section 3 and Charleston USGS gage; (middle) average daily gradient, BLM Well No. 5 to 4 at Lewis Springs; (bottom) rainfall depth and average daily temperature recorded at the Lewis Springs mesquite tower.

which to compute the water balance. DOY 101–191 was selected for the water balance calculation. During this period of time there was very little rainfall (<12.5 mm) and no apparent runoff in response to rainfall in this or upstream portions of the San Pedro basin. C/W and mesquite vegetation were thus assumed to be transpiring only groundwater from the alluvial or regional aquifer. The isotope analysis presented in Snyder and Williams (2000) is also consistent with this assumption. Small changes in surface soil moisture were accounted for in the water balance but they were minor compared to C/W and mesquite ET fluxes (roughly 8% of the fluxes). By utilizing this time period for the water balance, the difficulty of plant water source partitioning between ground and near-term surface water sources is therefore largely avoided.

A discussion on the data sources and procedures used to estimate each of the water balance components and an approximate estimate of their uncertainty for the DOY 101–191 period follows. Uncertainty estimates were determined by computing the standard error of the function for each water balance component (Brinker, 1969; Wolf, 1980). For a general function  $z = f(a, b, c, \dots, p)$ , where  $a, b, c, \dots, p$  are independently observed quantities, and the standard error of the function  $\sigma_z$  was computed as

$$\sigma_z = \sqrt{\left[\frac{\partial z}{\partial a}\sigma_a\right]^2 + \left[\frac{\partial z}{\partial b}\sigma_b\right]^2 + \left[\frac{\partial z}{\partial c}\sigma_c\right]^2 + \dots + \left[\frac{\partial z}{\partial p}\sigma_p\right]^2} \quad (7)$$

where  $\sigma_a, \sigma_b, \dots, \sigma_p$  are the standard errors of each component. Measurement errors for direct measurements such as stream stage or vegetation areas were estimated based on knowledge of the measurement devices or methods employed. Standard errors from regression estimates such as stage–discharge ratings or model estimates such as the P–M model for C/W transpiration were employed in the standard error function. For those components requiring spatial scaling, the areas of various classes from Lewis Springs to Charleston are contained in Column 2 of Table 1.

The inflow and outflow volumes ( $Q_{in}$  and  $Q_{out}$ ) were obtained from continuous stage measurements and stage–discharge rating curves at Lewis Springs

and Charleston. The discharge values in [ $L^3T^{-1}$ ] were then integrated from DOY 101 at 00:00 h to DOY 191 at 00:00 h. The uncertainty for these volumes was estimated by assuming that the standard error of estimate in the rating curves at Charleston was equal to that at Lewis Springs ( $0.005 \text{ m}^3 \text{ s}^{-1}$  or  $0.192 \text{ ft}^3 \text{ s}^{-1}$ ) and the error in stage was 3 mm.

The volume of water evaporated from the stream water surface ( $E_{ws}$ ) was computed as follows. For each day of the water balance, the Penman potential evaporation was computed using meteorological data from the Lewis Springs mesquite site (Scott et al., 2000) in millimeters per day. This procedure assumes that the meteorological conditions observed at this location are representative of the entire reach. Additional meteorological observations at the Escapule Wash sap flow site, approximately 7 km north of the Lewis Springs, were used to evaluate this assumption. Common periods of data collection at the two sites occurred in 1997 for DOY 161.5–163.7, 191.7–193.4, and 219.5–221.7. For these periods, the difference in the mean air temperature between the two sites was  $0.50^\circ\text{C}$ , with a correlation coefficient of 0.98. Vapor pressure (kPa) was also very similar at the two sites. The mean difference between the two sites was 0.10 kPa, with a correlation coefficient of 0.97. Thus, the mesquite tower measurements at Lewis Springs are fairly representative over the distance between these two sites.

Using measured radiation from the open mesquite tower results in a much higher estimate of Penman potential evaporation than in the shaded stream areas. To account for shading of the open water surface by streamside vegetation a factor of 0.6 was applied to the Penman potential evaporation estimates. This quantity was multiplied by the water area in Table 1. It should be noted this area was obtained from remotely sensed data acquired in May of 1996. The surface area of the stream exposed to the atmosphere obviously fluctuates with changes in stream stage. However, the estimate based on the area determined from May 1996 is the best available. Given the lack of measurements of the stream surface area over time, a relatively large uncertainty of 40% was assigned to stream surface area and a 20% uncertainty was estimated in the calculation of the Penman potential evaporation.

The volume of water added to the control volume in the form of precipitation on the stream water surface

Table 1  
Selected vegetation class areas for various San Pedro River reaches (area in hectares)

Land cover type	Lewis Springs to Charleston gage <sup>a,b</sup>	Hereford to Fairbanks <sup>b,c</sup>	US/Mexico border to Tombstone gage <sup>b</sup>	Palominas Gage to Charleston gage <sup>b</sup>	Charleston gage to Tombstone gage <sup>b</sup>	ADWR (1991) US/Mexico border to Tombstone gage
Riparian woodland (CW/W)	96	435	540	435	85	558
High-density mesquite	41	490	515	145	350	630
Low-density mesquite	101	545	580	335	245	1164
Sacaton	81					
Scrub	220					
Bare	12					
Water	2.0	4.6	4.7	3.6	1.1	N/A

<sup>a</sup> Corridor region for water balance computations.

<sup>b</sup> See Appendix A for data source and methods description.

<sup>c</sup> Riparian corridor region covered by four thermal remote sensing overflights.

( $P_{\text{pt}_{\text{ws}}}$ ) was also derived by scaling the rainfall measured at the mesquite tower by the remotely sensed estimate of stream surface area. As in the case of  $E_{\text{ws}}$ , a large uncertainty of 40% was assigned to the remotely estimated water area. Because rainfall typically has a high degree of spatial variability, a 40% error was assigned to the measured rainfall depth. Precipitation falling on vegetation in the riparian corridor was not considered in the water balance. None of the rainfall events recorded during DOY 101–191 exceeded 5 mm with largest being 4.3 mm over a 4.34 h period. It was assumed that this light rainfall was intercepted by vegetation or fell on the soil surface such that it quickly evaporated and did not substantially increase soil moisture. However, the observed rainfall amounts were assumed to satisfy ET demands of the vegetation. The rainfall totals were subtracted from the total estimates of transpiration from the C/W and the mesquite.

The net volume of groundwater inflow ( $\text{GW}_{\text{net}}$ ) from the regional aquifer (deep basin sediments) was determined by computing the gains during a period of no transpiration and then indexing that gain by the water surface potential (head) gradient between a deep well in the regional aquifer and a shallow well at the top of the regional aquifer. Indexing to the head gradient was assumed to account for changes of inflow over time into the control volume from the regional aquifer (see middle portion of Fig. 4). By selecting a dry pre-green-up period, the riparian ET terms are assumed to be zero. If the selected period of time has no rainfall and assuming the residual term is zero, Eq. (6) can be solved for  $\text{GW}_{\text{net}}$  as

$$\text{GW}_{\text{net}} = Q_{\text{out}} - Q_{\text{in}} + E_{\text{ws}} + \Delta\text{Storage} \quad (8)$$

By utilizing field observations and examination of the stream discharge and groundwater level data available, the period DOY 80–90 was selected to compute  $\text{GW}_{\text{net}}$ ,  $Q_{\text{in}}$ , and  $Q_{\text{out}}$ . Evaporation from the stream water surface ( $E_{\text{ws}}$ ) was computed as discussed above. The change in storage term results from a draining of the alluvial aquifer, a decrease in stream stage, and gains or losses of unsaturated soil moisture. The change in storage was computed for three portions of the control volume as

$$\Delta\text{Storage} = \Delta S_{\text{post}} + \Delta S_{\text{pre}} + \Delta S_{\text{st}} + \Delta\text{SM} \quad (9)$$

In this equation,  $\Delta S_{\text{post}}$  is the change in storage of the post-entrenchment alluvial aquifer which lies in a narrow portion of the riparian floodplain adjacent to the currently active channel (see middle portion of Fig. 3). The extent of this aquifer was obtained from Demsey and Pearthree (1994).  $\Delta S_{\text{pre}}$  is the change in storage within the pre-entrenchment alluvial aquifer. The area of this aquifer was determined by subtracting the area of the post-entrenchment aquifer from the overall riparian corridor area described in Appendix A (also see middle portion of Fig. 3).  $\Delta S_{\text{st}}$  is the change in storage within the stream. This was computed by multiplying the remotely sensed stream area by the average change in stage at Lewis Springs and Charleston at the beginning and end of the DOY 80–90 time period.  $\Delta\text{SM}$  is the change in unsaturated soil moisture. For the DOY 80–90 time period, this term was assumed to be zero as groundwater flow was upward into the alluvial aquifer and largely disconnected from the unsaturated zone that was monitored for soil moisture changes.  $\Delta\text{SM}$  was considered in the DOY 101–191 water balance as it could readily contribute to transpiration and evaporation losses out of the control volume. Readings from water content reflectometry probes at depths of 10, 25, 50 and 100 cm in soils near the mesquite and sacaton Bowen ratio towers were used to estimate changes in soil moisture (Scott et al., 2000).

The change in storage of the post- and pre-entrenchment aquifers was computed by multiplying the area of these aquifers times the drop in water table within each aquifer times the specific yield of the aquifer. The specific yield is the volume of water released from a porous media for a unit drop of the water table per unit area. The specific yield for the pre-entrenchment alluvium was set to 0.15 following Corell et al. (1996). The coarser material making up the post-entrenchment alluvium justified a higher specific yield. A value of 0.25 was selected based on the optimized value of 0.2 obtained by MacNish et al. (2000). The 0.2 value represented an average specific yield for the Lewis Springs area. The intensive measurement area at Lewis Springs contained roughly equal areas of post- and pre-entrenchment alluvium. The specific yields could be obtained with more accuracy with a pump test, but this was not feasible at Lewis Springs due to limited depth of saturated thickness within the alluvial aquifer. This was not considered a critical shortcoming as MacNish et al. (2000)

demonstrated that specific yield was the least sensitive parameter in their localized water balance computation around Lewis Springs. A similar computation for change in storage was made over DOY 101–191. The uncertainty in this term was estimated by assuming the errors in the areas of the alluvial aquifers were up to 15%, the change in water table measurement errors were roughly 5 mm and the specific yield error was 0.05. Soil moisture storage changes were also scaled using land cover class areas. The integrated change in soil moisture at the mesquite tower was multiplied by the high- and low-density mesquite land cover areas. The soil moisture changes at the sacaton tower were assumed to apply to the sacaton, scrub and bare land cover class areas and the changes at the mesquite tower were assumed to apply to the C/W areas. Based on calibration of the soil moisture instruments an error of 2% of volumetric soil moisture was assumed. The error in the depth of probe placement was assumed to be 1 cm.

The changes in water table depth were determined by selecting a set of piezometers within each of the aquifers and averaging the change in depth from the beginning to end of the time period examined. The piezometers selected to determine the change in head level for the pre-entrenchment aquifer were WNF 13, WMF 13, WSF 14, WMC 14, and ENC 13. For the post-entrenchment aquifer, piezometers EMC 10, EMF 10, ESC 10 and ESF 11 were used (see MacNish et al., 2000 for more detail). Using this information and Eq. (8),  $GW_{\text{net}(80-90)}$  (DOY 80–90) was  $73\,200\text{ m}^3$  which is equivalent to a rate of gain of  $0.0847\text{ m}^3\text{ s}^{-1}$  over the 10 days period. For the same period of time, the average gradient between BLM well #4 and BLM well #5 was computed ( $\nabla(4, 5)_{(80-90)}$ ). These wells are located on cross-section 3 at Lewis Springs with well #4 finished at a depth of roughly 7 m and well #5 finished at a depth of roughly 54 m.

The net groundwater gain during the water balance period from DOY 101 to 191 was computed by adjusting the pre-green-up gain with the ratio of the observed to pre-green-up gradient between wells 4 and 5 as follows:

$$GW_{\text{net}(101-191)} = \sum_{i=101}^{191} GW_{\text{net}(80-90)} \left[ \frac{\nabla(4, 5)_i}{\nabla(4, 5)_{(80-90)}} \right] \quad (10)$$

This was done in an attempt to account for changes in the net groundwater gain resulting from time-varying changes in the regional aquifer. The uncertainty associated with this term was computed by substituting the standard error for the Lewis Springs stage–discharge rating for  $GW_{\text{net}(80-90)}$  in Eq. (10). Error in difference in head measurements and the separation distance between the deep and shallow well were assumed to be 0.005 and 0.5 m, respectively.

The volume of water transpired by the C/W forest ( $T_{C/W}$ ) was estimated by summing the average daily values of transpiration obtained from the calibrated P–M model scaled by the remotely sensed area for the riparian woodland (Column 2 of Table 1). Scaling in this fashion implies several assumptions: (1) the meteorological measurements made at the Lewis Springs mesquite tower are representative of the entire reach; (2) the trees as well as the relative proportions of young and old trees sampled at Lewis Springs are representative of the entire reach. The last assumption was required as the remotely sensed data were not able to distinguish old from new growth. The uncertainty in this term is relatively large due to the multiple measurements and estimates that are made in scaling from the tree, to stand, to riparian corridor level. Errors in the scaling process include: the standard error in the sapwood area versus tree diameter regression, the standard error of the (sap flux/unit sapwood area) measurements, the daily error in the P–M model calibration, and the estimated error in the remotely sensed area of riparian woodland (2%, see Appendix A).

The volume of water evaporated and transpired by the mesquite trees ( $ET_m$ ) was determined by summing the average daily values of mesquite ET multiplied by the area for this vegetation class. As noted in Appendix A, the uncertainty associated with the area of this vegetation class is estimated to be 2–5% and the larger figure was used in the error calculation. The Bowen ratio ET estimates are assumed to be accurate to within 20%.

## 5. Results and discussion

Several preliminary results regarding sacaton grass ET water sources and the ability of remotely sensed data to detect changes in the hydrologic regime will be briefly discussed. More substantial results are

presented in individual subsections. Section 5.1 pertains to mesquite ET and Section 5.2 pertains to results regarding the C/W transpiration measurements, their scaling and calibration of the P–M model. Section 5.3 contains the results of the water balance computations at both the stand and corridor level. Finally, in Section 5.4, results and discussion regarding the scaling to these riparian ET estimates to the overall corridor are presented.

The first brief result, from Scott et al. (2000) regarding the sacaton grass, resulted in a simplification of the approach employed herein. While the sacaton grasslands were originally envisioned to utilize groundwater, Scott et al. (2000) concluded that ET from most of the sacaton in the Lewis Springs portion of the San Pedro originates almost entirely from near-term precipitation and from soil moisture storage. They noted that the 1997 yearly precipitation at the sacaton site was 247 mm with an increase of 8 mm of soil moisture, while the total evaporation loss measured at the sacaton tower was 272 mm (see Figs. 3 and 4a of Scott et al., 2000). Assuming a 20% error in the Bowen ratio and soil moisture measurements, and a 10% in the rainfall measurements, it was assumed that all evaporative losses from the sacaton originated from rainfall and soil moisture changes. Therefore, groundwater extraction via transpiration from the sacaton grass was not considered significant, and was not considered as part of the water balance computations for the entire corridor.

The second result regarding the remotely sensed thermal data also simplified the approach to the overall riparian corridor ET estimation. It was hypothesized that the riparian vegetation in the well-watered perennial reaches would exhibit significantly cooler surface temperatures due to greater transpiration than more highly stressed vegetation in intermittent reaches of the river. If true, this would justify using the remotely sensed surface temperature data to spatially partition the riparian corridor to differentially estimate ET when reaches of the river became intermittent. To test this hypothesis, remotely sensed surface temperatures of several well-defined cottonwood clusters at nearly identical times near Lewis Springs and the Boquillas Ranch were examined for the April, July, and August flight dates. The limited data indicated a relatively small increase in the temperature difference (0.7–1.2°C) between the dry Boquillas reach and the

flowing Lewis Springs reach for the July overflight. Even though ground observations noted stressed vegetation and a loss of leaves at the dry intermittent site, the hypothesized increase in surface temperature may have been masked by understory conditions or the resolution of the sensor. Partitioning the riparian corridor for differential computation of riparian ET based on the acquired thermal remote sensing data was therefore not justified.

### 5.1. Mesquite ET

To scale the Bowen ratio measurements from the mesquite tower using the classified land cover area, it was necessary to derive mesquite ET estimates for the equivalent of 100% mesquite cover. To accomplish this, the following simple linear partitioning of the fluxes at the mesquite tower was assumed:

$$BR_m = (ET_m + I_m)A_m + (ET_{ssb} + I_{ssb})A_{ssb} \quad (11)$$

where  $BR_m$  is the measured Bowen ratio flux at the mesquite tower,  $ET_m$  the mesquite ET,  $I_m$  the amount of intercepted rainfall contributing to the fluxes measured at the Bowen ratio tower,  $A_m$  the percentage area of mesquite contributing to the fluxes measured at the Bowen ratio tower, and  $ET_{ssb}$ ,  $I_{ssb}$ , and  $A_{ssb}$  are comparable quantities for the sacaton, scrub and bare areas contributing to the fluxes at the mesquite Bowen ratio tower.

Scott et al. (2000) estimated the percentage area of mesquites contributing to the measured fluxes at the mesquite Bowen ratio tower was approximately 50%, while sacaton, scrub and bare areas comprised the other 50%. For this analysis, it was assumed that the quantity  $(ET_{ssb} + I_{ssb})$  was equal to the evaporative fluxes measured at the sacaton Bowen ratio tower as these three cover classes comprised virtually the entire area contributing to the fluxes measured at that tower. Interception was assumed to equal to first 3 mm of rainfall of any event based on measurements by Tromble (1983) on desert tarbush. Given the large uncertainties in defining the source areas for flux measurements, both of the percentage area estimates in Eq. (11) were assigned errors of 50%.

The estimates obtained for mesquite ET for the water balance period (DOY 101–191) and for the entire growing season (DOY 101–294) were 184 and

402 mm, respectively. Partitioning of mesquite ET derived from surface water or groundwater sources was not possible with the measurements made. The entire-scaled mesquite ET estimate for both the water balance and the growing season was assumed to be derived solely from groundwater. This appears to be a reasonable assumption during the pre-monsoon water balance period, but limited measurements presented in Snyder and Williams (2000) indicate that the mesquite can readily use surface water when it becomes available. During the monsoon, after significant rains and runoff events occurred, several mesquites that Snyder and Williams (2000) measured, were able to derive over 50% of their transpired water from surface sources. Therefore, the growing season estimate of the amount of groundwater used by mesquites obtained from the mesquite tower is conservatively large (i.e. if the mesquites are able to use surface water during the monsoon then less groundwater from the regional aquifer will be used). Clearly more detailed isotopic and flux measurements (given adequate time and resources) must be made on a variety of mesquites to fully understand their water sources and transpiration quantities.

### 5.2. *C/W transpiration and P–M model calibration*

Schaeffer et al. (2000) present the sap flux measurements and results for estimating *C/W* transpiration at the trees and patch scale. The results discussed herein focus on scaling these measurements and our ability to model them. In examining the patch level results, it was found that the variance in sapwood area to canopy area was relatively large across the patches. This was in part attributed to the differences in canopy structure between the young or newly established patches and the older patches. Schaeffer et al. (2000) concluded that the differences between the young and old patches in water use per unit canopy area were significantly different. However, at the patch scale, good agreement existed between the sap flow estimates of *C/W* transpiration and independently derived estimates of ET from the scanning Raman LIDAR. Both Cooper et al. (2000) and Eichinger et al. (2000) found an RMSE between the sap flow and LIDAR-based ET estimates of approximately  $0.03 \text{ mm h}^{-1}$  or  $0.36 \text{ mm per day}$  assuming a nominal 12 h of transpiration per day. Another factor, noted above, which makes

comparison across the patches problematic is the uncertainty in estimating the area of the patch. For the relatively small patches ( $444\text{--}1985 \text{ m}^2$ ), the ratio of patch perimeter to area is relatively large. This uncertainty could also have contributed to the high variance in sapwood area to canopy area across the patches. As noted in Section 4.1, we assumed that sampling a larger number of trees to scale from the patch to stand level provided a more certain estimate of the canopy area as well as a more representative sample of trees.

The sap flux estimates of *C/W* transpiration scaled to the stand level on a per unit canopy area basis for DOY 158 and 159 of the 2238 trees at Lewis Springs are illustrated in left-hand portion of Fig. 5. The error bands for these estimates computed using Eq. (7) are also included in this portion of the figure. These error estimates include the errors associated with the sapwood area versus tree diameter regression and the standard error of the sap flux measurements. Also included in the right-hand side of this figure is a comparison between stand level *C/W* transpiration at the well-watered Lewis Springs site and the ephemeral Escapule Wash site for DOY 192. The fluxes for the stressed Escapule site are less than half of those at Lewis Springs. However, it should be noted that these trees are in a side wash approximately 250–300 m away from, and substantially higher than, the main channel of the San Pedro. These trees have less access to groundwater than those near the main channel and lower in the floodplain. This situation is not common in the reach between Lewis Springs and Charleston but it does demonstrate the large variation of sap flux depending on the trees access to groundwater.

The scaled stand level estimates of *C/W* transpiration at Lewis Springs for each SMP (e.g. the left-hand side of Fig. 5) were used to compute the bulk canopy level resistance using Eq. (5) as described in Section 4.2.1. This procedure resulted in an average daily calibrated bulk canopy resistance for each SMP. A constant daily average value of canopy resistance was used in subsequent computations even though stomatal resistance (and hence canopy resistance) is known to fluctuate diurnally. For each multi-day SMP, an average canopy resistance was obtained by averaging the daily calibrated resistances for each day of the SMP. For example, the average daily resistances computed for DOY 191, 192, 193, and 194 were 123, 144, 192, and  $182 \text{ s m}^{-1}$ , respectively. The average value of

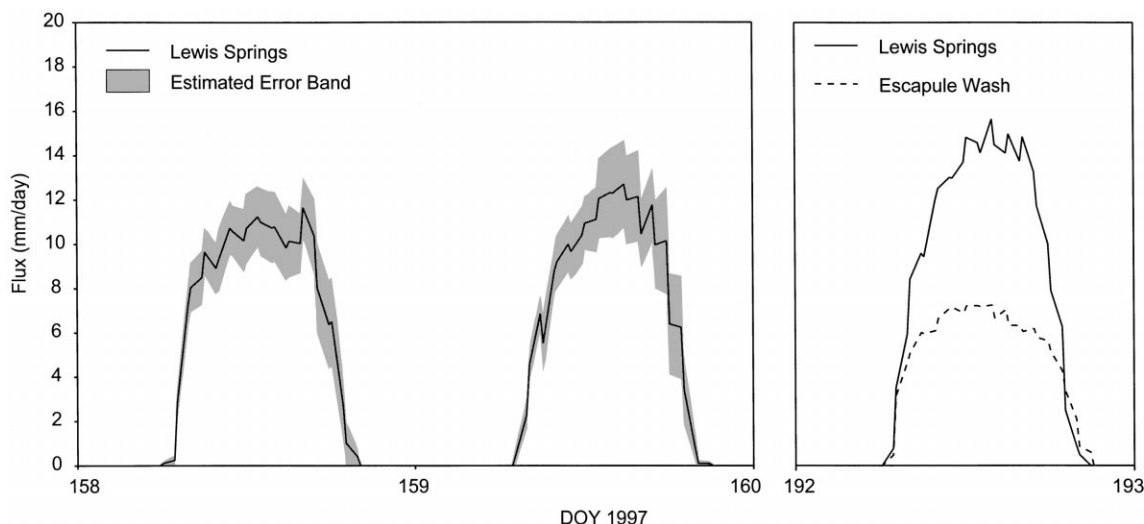


Fig. 5. (Left) scaled sap flow estimates over the 600 m Lewis Springs reach of C/W transpiration for DOY 158 and 159 with estimated error bands; (right) comparison of scaled Lewis Springs versus the ephemeral channel Escapule Wash reach for DOY 192.

$160 \text{ s m}^{-1}$  for the DOY 191–194 measurement period were utilized to interpolate a seasonal curve of canopy resistance that was used in the daily estimation of C/W transpiration throughout the growing season. No diurnal changes were modeled. Even with these simplifications, the calibrated model was able to largely capture the fluctuations in the scaled sap flux measurements. This is illustrated in Fig. 6. In this figure, the scaled sap flux measurements and those computed from the calibrated P–M model for each of the five synoptic measurement periods are plotted as a function of time. The same data are also depicted as scatter plots in Fig. 7. The top portion of this figure contains the P–M model estimates for each 20 min time step versus the interpolated (from 30 min intervals) scaled sap flux measurements. The coefficient of variation ( $R^2$ ) and RMSE for these data are 0.91 and 1.34 mm per day, respectively. The lower portion of Fig. 7 is a one to one scatter plot of the modeled versus measured sap flux data for each day of scaled sap flux measurements. On a daily time scale, good agreement is also apparent with  $R^2 = 0.94$ , and the RMSE = 0.36 mm per day. The ability of this simple, although calibrated model, to capture much of the variability of the measurements using the simple synoptic daily average resistances indicates that transpiration is primarily controlled by the available energy and not the trees' stomata on a daily basis.

Generally, the average daily canopy resistances computed from the scaled sap flux measurements were relatively constant across the synoptic measurement periods (the growing season), except during early and late periods of green-up and leaf drop. This is to be expected for vegetation that is not water limited. Based on prior studies, the calibrated canopy resistances are also realistic. Hall and Roberts (1990) presented a compilation of maximum stomatal conductance from 25 genera of broadleaf trees found in the United Kingdom for a wide range of old and new trees. The range of values they report converted to resistances ranged from a minimum of  $111 \text{ s m}^{-1}$  to a maximum of  $833 \text{ s m}^{-1}$ . Shuttleworth (1989) presented a collection of data from various studies showing the diurnal variation of canopy conductance for a wide variety of trees. In this case, the values ranged from 66 to  $1000 \text{ s m}^{-1}$ . In addition, Magnani et al. (1998) estimated the seasonal minimum canopy resistance of 54 and a mean value of  $200 \text{ s m}^{-1}$  from a mature beech forest. It was thus assumed that the calibrated bulk canopy resistances were physically plausible.

To apply the P–M model throughout the growing season, bulk canopy resistance values for each day are required. Intersynoptic period canopy resistances were based on a linear interpolation between the calibrated values obtained during the SMP. The

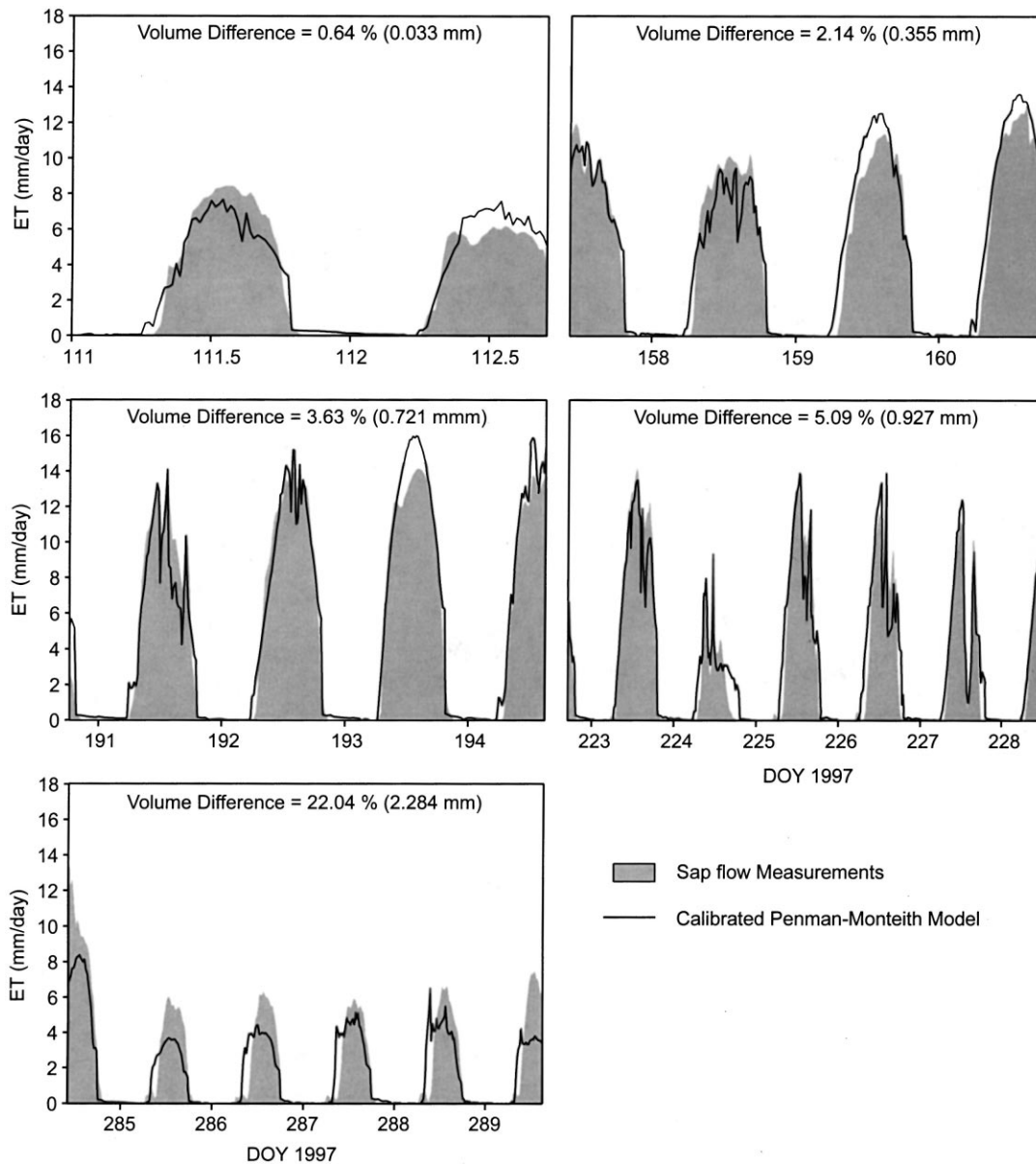


Fig. 6. Comparison of calibrated P-M model for C/W transpiration versus scaled sap flow estimates for each of the 1997 intensive measurement periods.

following conditions were also applied. To stop transpiration at nighttime (the stomata close in the absence of solar radiation), a value of  $r_c = 5000 \text{ s m}^{-1}$  was used when the value of solar radiation was less than  $10 \text{ W m}^{-2}$ . DOY 104 was assumed to be the start of the cottonwood season (based on visual observations

of bud burst) and DOY 294 was assumed to be the end of the cottonwood's transpiration activity. To represent senescence of the trees, the canopy resistance was set to  $1000 \text{ s m}^{-1}$  for computations made prior to DOY 104 and after DOY 294. The seasonal evolution of the canopy resistances derived from Eq. (5) with the

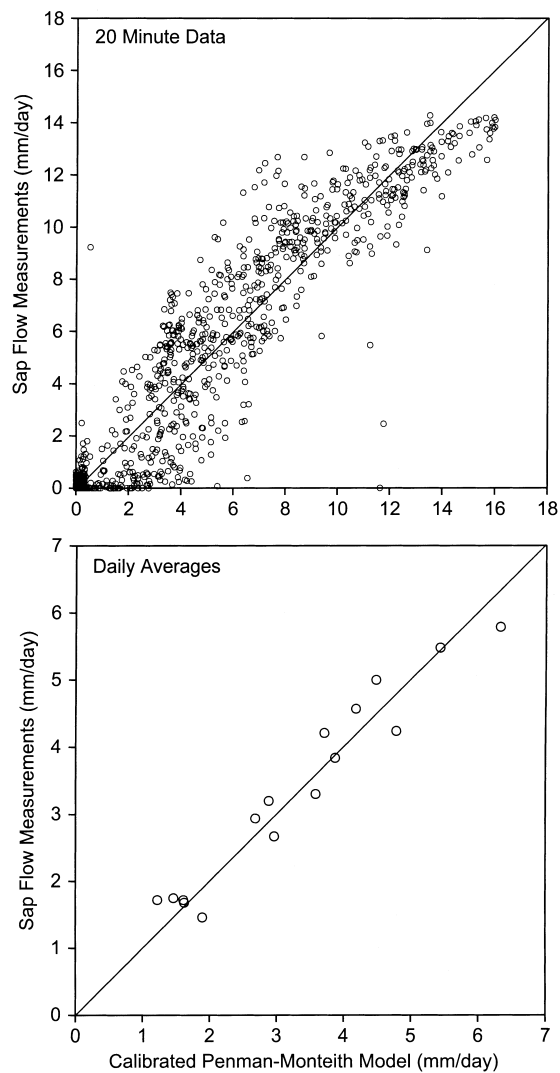


Fig. 7. Comparison of the 20 min (top) and average daily (bottom) C/W transpiration as estimated by scaled sap flow measurements and estimates derived from the calibrated P–M model.

above-noted conditions are contained in Table 2. In this table, the italic values indicate the days on which an average daily bulk canopy resistance was computed from the scaled sap flux measurements using Eq. (5) over all days of the intensive SMP.

### 5.3. Water balance closure and uncertainty estimates

Each of the independently derived components of the DOY 101–191 water balance in Eq. (6) are tabulated in Table 3. The primary assumptions made in estimating each of the water balance components are collected and restated here: (1) Water use by the sacaton grass and understory of the C/W is derived from precipitation and soil moisture only; (2) C/W and mesquite use only groundwater; (3) Limited precipitation falling on C/W and mesquite (<3 mm) was all intercepted and subsequently evaporated; (4) The surface area of the river was constant as estimated from May 1996 remotely sensed data and evaporation from the river was 60% of Penman potential evaporation.

Table 3 also contains uncertainty estimates for each water balance component as well as the measurement or method used to estimate each component. By substituting the values in Table 3 (Column 2) into Eq. (6) a residual, or closure of the water balance, of  $-57\,800\text{ m}^3$  was obtained. The percentage error in the water balance was computed by dividing the residual by the total of the input components of the balance resulting in an error of  $-5.2\%$ . As noted above, when interpreting this error of closure it must be kept in mind that compensating errors in various water balance components may result in a smaller overall error percentage. Future work and improved measurements discussed below would result in reduced uncertainty estimates. Even with these caveats, the relatively small error in the water balance lends confidence

Table 2  
Seasonal change in canopy resistance used in the model<sup>a</sup>

Day of year	104 <sup>b</sup>	<i>111</i>	125 <sup>c</sup>	<i>158</i>	<i>192</i>	<i>225</i>	<i>284</i>	<i>287</i>	294 <sup>b</sup>
Canopy resistance ( $\text{s m}^{-1}$ ) <sup>d</sup>	1000	<i>391</i>	186	<i>186</i>	<i>160</i>	<i>160</i>	<i>160</i>	<i>631</i>	1000

<sup>a</sup> Italic values are taken from average daytime (09:30–14:30 h).

<sup>b</sup> DOY 104 and 294 values represent tree senescence.

<sup>c</sup> DOY 125 value was estimated from the fact that it took about 2 weeks for the canopy to fully leaf out after DOY 111.

<sup>d</sup> Resistances calculated from the scaled sap flux measurements using Eq. (5).

Table 3

Water balance results, Lewis Springs to Charleston, DOY 101–191 (see Eq. (6) for definition of water balance components), and associated uncertainty estimates

Component	Volume of water (m <sup>3</sup> )	Uncertainty estimate	Measurement or estimate method
$Q_{in}$	438000	~1000 m <sup>3</sup> or 0.22%	Stream stage and rating table
$GW_{net}$	664000	~109 000 m <sup>3</sup> or 16%	Eq. (8)
$Ppt_{ws}$	200	~100 m <sup>3</sup> or 50%	Lewis Springs raingauge
$Q_{out}$	-766000	~1700 m <sup>3</sup> or 0.22%	Stream stage and rating table
$T_{C/W}$	-382000	~13 000 m <sup>3</sup> or 3.4%	Calibrated P–M model (Eq. (1))
$ET_m$	-263000	~153 000 m <sup>3</sup> or 58%	Eq. (11)
$E_{ws}$	-8000	~3700 m <sup>3</sup> or 46%	60% of Penman potential ET
$\Delta Storage$	259000	~73 000 m <sup>3</sup> or 28%	Eq. (9)
Residual ( $\epsilon$ )	-57800	~202 000 m <sup>3</sup> or 342%	Eq. (6)
Error (%)	-5.2		(Residual/total inputs) $\times$ 100

to the models and methodology for describing C/W transpiration and mesquite ET.

#### 5.4. Scaling riparian ET to larger areas

The P–M model for C/W transpiration and the mesquite ET measurements were then scaled spatially over several different reaches to enable comparisons to riparian ET estimates obtained from groundwater modeling studies by Corell et al. (1996). The estimates by Corell et al. (1996) represent annual average values. To obtain annual estimates from the ET models and measurements described herein, the meteorological conditions measured at the Lewis Springs mesquite site were used over the observed growing season at Lewis Springs (DOY 101–294). Spatial extrapolation over the entire corridor requires the assumptions noted above (Section 5.3) as well as assuming uniform meteorology over the corridor. Temporal extrapolation over the entire growing season invokes the following major assumptions: (1) that the C/W and mesquite trees water source remains groundwater throughout the monsoon season where significant rainfall and runoff occurred (see top and bottom parts of Fig. 4), and (2) the vegetation for the entire riparian reach behaves similarly to the vegetation at Lewis Springs. Because of these assumptions, the resulting 1997 annual riparian ET estimates for groundwater use are likely to be conservatively high. Snyder and Williams (2000) concluded that the near-stream mesquites readily change water sources to rainfall and runoff when it becomes

available which would decrease groundwater use. In addition, it was observed that in significant portions of the riparian corridor, streamflow became intermittent prior to the monsoon near Palominas and north of Charleston. If the sap flux transpiration estimates from the ephemeral Escapule Wash site (right-hand side of Fig. 5) are an indication of the transpiration rates in a water-stressed environments, then the estimates scaled from the perennial Lewis Springs to Charleston reach would also be high. On the other hand, it was observed that upper reaches, from roughly the border to Hereford, greened up several weeks earlier than the Lewis Springs area. This was attributed to cold air drainage from the Huachuca Mountains affecting areas downstream of the Hereford area. The earlier green up in the upstream reaches would result in riparian ET estimates from groundwater that are higher than those from the extrapolated model.

Annual riparian ET was estimated over two common river segments also used by Corell et al. (1996) to facilitate a more direct comparison (Table 4). In addition, annual riparian ET was estimated over the corridor with classified land cover imagery from the US/Mexico border to the Tombstone USGS gage. The first common segment spans the reach from the USGS stream gage at Palominas to the gage at Charleston, and the second from the Charleston gage to the Tombstone gage. Corell et al. (1996) defined ET estimates as “the amount of groundwater discharge to the San Pedro and Babocomari Rivers that is intercepted by riparian use, by agricultural pumping, and to a lesser extent by other pumpage

Table 4  
Comparison of annual riparian ET estimates from groundwater sources for various river reaches

Reach	Groundwater model: steady-state (ca. 1940) <sup>a</sup>		Groundwater model: transient for 1981–1986 <sup>b</sup>		Scaled P–M for C/W and Bowen ratio for mesquite	
	(m <sup>3</sup> )	(ac-ft)	(m <sup>3</sup> )	(ac-ft)	(m <sup>3</sup> )	(ac-ft)
Palominas to Charleston	4471400	3625	4193800	3400	4941000	4005
Charleston to Tombstone	2343600 <sup>c</sup>	1900 <sup>c</sup>	3453700 <sup>c</sup>	2800 <sup>c</sup>	2981000	2417
Southern boundary to Tombstone US/Mexico border to Tombstone	9362100 <sup>c</sup>	7590 <sup>c</sup>	8881000 <sup>c</sup>	7200 <sup>c</sup>	8130000	6591

<sup>a</sup> Corell et al. (1996), Fig. 7.

<sup>b</sup> Scaled from Corell et al. (1996, Figs. 9–11).

<sup>c</sup> Excludes ~740 000 m<sup>3</sup> (600 ac-ft) of Bobocomari River ET.

in the basin (p. 24)". Agricultural pumping was not included in this study. However, it was known that no agricultural pumping of any significance occurred between the Charleston and Tombstones gages in 1997. For their steady-state model analysis (ca. 1940), they estimate the ET from the Babocomari River to be approximately 740 000 m<sup>3</sup> (600 ac-ft) which is included in their ET estimates between the Charleston and Tombstone gage. Since the present study did not model riparian ET from the Babocomari River, this value was subtracted from the Corell et al. (1996) model estimates (these values were not available for the transient groundwater model runs). The estimated annual riparian ET estimates for the two studies and the various reaches are contained in Table 4.

The most closely comparable figures are those for the reach between the Charleston and Tombstone USGS gages. In this reach there is no significant agricultural pumping so the groundwater model estimates should reflect those of riparian ET alone. The values for this reach indicate that the 1997 riparian ET estimated from the methods presented herein is roughly 86% of the groundwater model-derived estimates over the 1981–1986 period. On a per unit area basis, the total 1997 C/W transpiration from the P–M model (755 mm) was also substantially lower than prior estimates. Using Blaney–Cridle evaporation-based methods, ADWR (1991) estimated a value of 1271 mm for cottonwoods in the San Pedro. Gatewood et al. (1950), based on the average of several measurement techniques in the lower Gila River valley, obtained annual cottonwood water use estimates of 1829 mm.

## 6. Summary

A series of field measurements were conducted over the 1997 riparian growing season to estimate riparian ET originating from groundwater over sections of the San Pedro River corridor. The approach utilized remotely sensed estimates of vegetation cover, local meteorological and energy balance measurements, and sap flow measurements of C/W transpiration. Sap flow measurements were scaled from a tree, to patch, to a stand level. Patch transpiration estimates agreed well with those estimated independently from scanning Raman LIDAR measurements on an hourly basis (Cooper et al., 2000; Eichinger et al., 2000). At the stand level, over a 122 m river reach at Lewis Springs, MacNish et al. (2000) demonstrated basic agreement between water balance and sap flux C/W ET estimates at a daily time scale for the April and June synoptic measurement runs. The sap flow measurements were then scaled to a stand level over a river reach of approximately 600 m. These scaled measurements were used to calibrate a P–M model of C/W transpiration by adjusting the canopy resistance term. On a daily basis over the five synoptic measurement periods the RMSE between the scaled sap flow measurements and the P–M model was 0.36 mm per day. With this model, C/W transpiration were extrapolated temporally throughout the growing season using locally measured meteorological quantities. Mesquite ET was scaled from Bowen ratio measurements at the Lewis Springs (Scott et al., 2000) site assuming all mesquite ET was derived from groundwater.

The validity of scaling the P–M C/W transpiration model and the mesquite ET was then assessed by carrying out a water balance over a 10 km reach between stream gages at Lewis Springs and Charleston over a 90-day pre-monsoon period. In this water balance, all components were estimated independently. For the 90-day water balance, the residual error of closure was  $-5.2\%$  of the input water volume. The uncertainty associated with the residual was  $18\%$  of the input water volume and  $31\%$  of the C/W transpiration and mesquite ET. The majority of the error originated from estimates of mesquite ET and the net groundwater inflow computation.

The mesquite ET error results largely from the uncertainty in specifying the number and area of mesquites contributing to the fluxes measured at the mesquite Bowen ratio tower. It does not include errors resulting from the assumption that all mesquite ET is derived from groundwater. The uncertainty could be reduced by improving the flux measurement instrumentation, making measurements over a much denser mesquite canopy, and conducting further isotopic studies to determine mesquite water sources. The large uncertainty in the net groundwater inflow term is largely the result of the estimation of evaporation from the water surface and the change in alluvial storage over the 10 days pre-green-up period (DOY 80–90). The error in these terms is carried into the net groundwater inflow computation in Eq. (10). The uncertainty in the net groundwater inflow term could be reduced considerably by better definition of the area of the pre- and post-entrenchment alluvium as well as the water table level change within the alluvium.

The measurements of riparian mesquite ET and model estimates of C/W transpiration were used to estimate riparian ET over the entire 1997 growing season for various reaches of the San Pedro. For the reach from the US/Mexico border to the USGS stream gage near Tombstone, the estimated annual volume of riparian ET was  $8\,130\,000\text{ m}^3$  (6591 ac-ft). For the reach between the USGS gages at Charleston and Tombstone the estimated riparian ET was  $2\,981\,000\text{ m}^3$  (2417 ac-ft). This quantity is roughly  $14\%$  less than estimates obtained from a transient groundwater model run from 1981 to 1986 (Corell et al., 1996) of  $3\,454\,000\text{ m}^3$  per year (2800 ac-ft per year).

These riparian ET estimates have important implications for basin water management. Based on the 1-year groundwater model run for 1990, Corell et al. (1996, p. 83) estimated that the current water balance in USPB is roughly  $6\,556\,000\text{ m}^3$  per year (5315 ac-ft per year) in deficit (more water being taken out of the basin than is being recharged). This same groundwater model estimates ET at  $9\,316\,000\text{ m}^3$  per year (7553 ac-ft per year). This not only represents riparian ET but also near-stream pumping. The expert study team of the trinational Commission on Environmental Cooperation (CEC, 1999) estimates the basin deficit at  $8\,633\,000\text{ m}^3$  per year (7000 ac-ft per year) at current levels of pumping. However, if the actual riparian ET is more closely approximated by the estimates presented herein (of the order of  $14\%$  less than the groundwater model ET estimate), the basin deficit, using the CEC, 1999 figure, is reduced by almost  $15\%$  from  $8\,633\,000\text{ m}^3$  per year (7000 ac-ft per year) to approximately  $7\,330\,000\text{ m}^3$  per year (5943 ac-ft per year). This assumes a  $14\%$  reduction in groundwater model riparian ET estimate of  $9\,316\,000\text{ m}^3$  per year (7553 ac-ft per year) which equals  $8\,012\,000\text{ m}^3$  per year (6496 ac-ft per year). Reduced riparian ET estimates could also impact groundwater recharge estimates. Recharge estimates are typically the residual of a water balance calculation in a steady-state groundwater model run. This will not be easy to assess as the basin is far from being in a steady-state at present. Further research is required to independently estimate groundwater recharge. However, if the actual riparian ET is more closely approximated by the proposed model and is consistently lower than groundwater model-derived estimates, management of the basin water resources to achieve an overall water balance will likely be made considerably easier.

## 7. Conclusions and recommendations

The following conclusions were drawn from this study.

1. Partitioning the riparian corridor for differential computation of riparian ET based on the acquired remote sensing data was not justified as the single-channel thermal remotely sensed data could not discern seasonal large-area hydrologic regime changes.

2. The calibrated P–M model of C/W transpiration, even with a set of simplifying assumptions, was able to largely capture the fluctuations in the scaled sap flux measurements.
3. The methodology to scale the sap flux measurements spatially with remotely sensed data and temporally with the P–M model provided good estimates of large area, long-term (pre-monsoon) transpiration based on stand and 10 km river reach water balance computations.
4. For 1997, the annual riparian ET estimates based on the methods presented herein were roughly 15% less than those derived from a regional groundwater model (Corell et al., 1996).

The following research and monitoring is recommended to reduce the uncertainty of the proposed riparian ET model estimates:

1. Carry out coordinated isotope, sap flow, energy balance, and water depth measurements on mesquites of different size and cover density to better quantify their ET and differentiate their water sources between groundwater and surface water throughout the growing season.
2. Install more meteorological stations in the upper, middle and lower portion of the riparian corridor to measure the quantities necessary to apply the P–M models in a more spatially distributed manner.
3. Install and monitor paired shallow piezometers at some spatial frequency along the riparian corridor to quantify the depth to water for various plant species to enable water source partitioning among plant species following the results of Snyder and Williams (2000) as well improve the estimates of storage change within the alluvial aquifers.
4. Carry out geophysical surveys to more accurately define the area of the pre- and post-entrenchment alluvial aquifers.
5. Conduct ground surveys to establish the relative extent and percentage coverage of young and old C/W stands to utilize the findings of Schaeffer et al. (2000) to apply different transpiration models to each type of stand.
6. Periodically obtain aerial imagery of the corridor and reclassify the land cover to account for changes due to fires, new growth, and the impacts of the reintroduction of beavers.

## Acknowledgements

Financial support from the USDA–ARS Global Change Research Program, NASA Grant W-18 997, NASA Landsat Science Team, Grant No. S-41396-F, USDA National Research Initiative Grant Program, Electrical Power Research Institute, Arizona Department of Water Resources, US Environmental Protection Agency, Office of Research and Development, CONACYT, ORSTOM, the French Remote Sensing Program (PNTS) via the VEGETATION projects and the ERS2/ATSR2 Project, and US Bureau of Land Management is gratefully acknowledged. Assistance was also provided in part by the NASA/EOS Grant NAGW2425, EPA STAR Graduate Student Fellowship Program, National Science Foundation, US Geological Survey, US Department of Energy contract W-7405-ENG-36, California Institute of Technology, Jet Propulsion Laboratory (NASA, EOS/ASTER), WAU (Wageningen Agricultural University, Netherlands), Cochise County Highway and Flood Control Department, and Ft. Huachuca; this support is also gratefully acknowledged. Support from the NSF–STC SAHRA (Sustainability of semi-Arid Hydrology and Riparian Areas) under Agreement No. EAR-9876800 is also gratefully acknowledged. Special thanks are also to the ARS staff located in Tombstone, AZ for their diligent efforts and to USDA–ARS, Weslaco, TX for pilot and aircraft support. We also wish to extend our sincere thanks to the many ARS and University of Arizona staff and students, and local volunteers who generously donated their time and expertise to make this project a success. The thorough review and helpful suggestions of the anonymous journal reviewers is also gratefully acknowledged.

## Appendix A. SALSA San Pedro riparian corridor vegetation classification

This section contains a description of how the vegetation classification of the USPB riparian corridor was obtained as part of the SALSA Program. This classification was accomplished using a combination of two kinds of remote sensing imagery, supported by extensive ground truth. Multi-spectral digital images of the riparian corridor were acquired by a TMS

deployed aboard a NASA Jet Propulsion Laboratory aircraft. High-resolution CIR photography was obtained over the same area with a 9 in. format mapping camera aboard a USDA–ARS aircraft from Weslaco, TX. The TMS imagery was acquired on two dates. The first date was on 29 May 1996 with 5 m resolution, and the second date was on 12 August 1997 with 3 m resolution. The CIR was flown on 13 August 1997 and had resolution of approximately 8 cm. Both TMS and one CIR collections were used because all three were required to acquire the greatest possible coverage of the riparian corridor. The CIR was also used to adjust and refine the classification of riparian woodland and mesquite.

The first step in the classification of the images was to correct for the TMS wide scan angle distortion which caused a pixel size difference and to georectify the images to a UTM, Clark 1866, NAD 27 coordinate reference system.

The riparian corridor classification extends from the US–Mexican border to a point 2 miles north of St. David and includes the area on either side of the river that was identified as the riparian corridor. The riparian corridor was defined using the USGS 1 arc second DEMs of the area and by visual interpretation of high-resolution CIR photography. The combination of the two techniques resulted in a corridor definition that was superior to attempts that utilized only one or the other of the two data sets. The approach was to select the corridor based on 6–9 m contour change from the river bottom based on the DEM. This area was then checked against high-resolution CIR photography. The area was then adjusted to more closely fit the riparian corridor based on photo interpretation of vegetation and terrain features. The resultant corridor boundary was then saved and used as a mask to subset the desired area from the classification. This technique is consistent with the methods recommended by the US Fish and Wildlife Service for defining riparian corridors.

TMS data has 10 reflected bands and two thermal bands. The two thermal bands (11 and 12) have the same bandwidth (8.5–12.5  $\mu\text{m}$ ) but band 11 is low gain and band 12 is high gain. The two data sets used here had good separation in band 11, but band 12 was somewhat saturated, the decision was therefore made to eliminate band 12 from the data sets. A normalized difference vegetation index (NDVI, bands 7, 5) was computed from each of the TMS images as well as a

normalized difference soil-adjusted vegetation index (NDSVI, bands 9, 5) and a soil enhancement (bands 10, 11). These indices were then co-registered with the other 11 TMS bands to provide a data set of 14 bands for classification.

The vegetation classification was accomplished using established techniques of both spatial and spectral analysis. For the spectral analysis, training sets were identified by using ground truth sites, photo truth sites, and feature space placement for the red and NIR bands. It was necessary to select over 100 training sites to achieve an accurate classification due to different soil backgrounds, vegetation health, cultural activity, and cloud shadow. Care was taken to select sites of known vegetation type that exhibited slightly different spectral properties due to shadow, soil background, or cultural activity (such as farming) even though they represented the same vegetation class. This was done in order to get the most accurate spectral classification possible. Due to the variations in imagery (especially cloud shadow) the images were subset into smaller areas before classification. Some of these subsets were developed to separate areas of bright sunlight from areas of cloud shadow, which required all new training sets. Other subsets were the result of spatial analysis and were extracted to eliminate signatures from areas where they did not belong. For example, the agriculture signature was removed from areas on the river where there was no agriculture but lush vegetation was classified as agriculture. Other subsets were extracted to eliminate riparian signatures from homogenous mesquite stands, and to eliminate mesquite signatures from the cottonwood willow gallery of the riparian woodland where they often accrued due to shadowing caused by the tree canopy. The classifications were run as supervised classifications using feature space and maximum likelihood. Once the classifications were complete they were co-registered together using the last overlay method.

A raster file of all mesquite pixels was then broken down into either low- or high-density based on the following procedure. The raster layer was imported into a grid file for ArcInfo (use of this and other commercial names in this paper is not intended as an endorsement of the product), then a window of  $9 \times 9$  pixels was passed over the file. If less than 75% of the pixels were mesquite then the center pixel, if mesquite, was classified as low-density mesquite. If

75% or more of the pixels were mesquite then the center pixel, if mesquite, was classified as high-density mesquite. If the center pixel was not mesquite then it was not changed. This layer was then co-registered with its parent classification. The result is a classification where mesquite now is either high- or low-density based on the above spatial properties.

The final step in the classification process was to extensively compare the classification with the CIR and make corrections where necessary. At this point the riparian wood (cottonwood and willow), and mesquite were adjusted and refined using photo interpretation techniques. This combination of spectral and spatial analysis took advantage of the strengths of these two techniques to produce a classification whose accuracy is outlined below.

#### A.1. Classification information

1. The classification resolution is 3 m.
2. The classes are riparian wood (cottonwood/willow), low-density mesquite, high-density mesquite, sacaton, scrub, bare soil, agriculture, and water.
3. The accuracy of the digital classification was assessed primarily by comparison with the high-resolution CIR photographs for all the riparian wood, areas, water areas and mesquite areas, as well as, many sacaton, scrub, and agricultural areas. Ground truth was carried out from Fairbanks to Hereford at 15 sites that each contained two or more of the classification signatures. The results of this ground truth were then used to correct errors in the classification.

The error of the classification is estimated to be no more than 1–2% for riparian wood, 2–5% for high- and low-density mesquites, and less than 10% for sacaton. The error of the other classes (agriculture, water, scrub, and bare soil) is estimated to be 10%. Agriculture refers only to irrigated crops that are growing. Fallow fields classified either as scrub or bare soil depending on their condition. These estimates are based on the aforementioned ground truth and extensive photo truth. The higher error associated with the mesquite is due to the transition from Chihuahua scrub with shrub mesquite to larger, more mature, mesquite. The higher error value associated with sacaton is the result of the

transition between sacaton and scrub, and the difficulty is visually identifying this boundary with photography.

4. Classification areas rounded to the nearest 10 ha (converted to the nearest 10 acres), except for classes under 10 ha.

From Palominas to a point 3.2 km (2 miles) north of St. David:

Riparian vegetation classes	Class area	
	In hectares	In acres
Riparian wood	620	1530
Low-density mesquite	830	2050
High-density mesquite	1470	3630
Sacaton	390	960
Agriculture <sup>a</sup>	30	70
Bare soil	70	170
Scrub	2090	5160
Water	5	12

<sup>a</sup> This does not include fallow fields. Plowed fallow fields classified as bare soil, and old fallow fields classified as scrub. Most of the irrigation crop area falls outside of the riparian corridor.

From the US–Mexico border to Palominas (this was done with visual interpretation as only the CIR was available for this area, therefore a distinction between low- and high-density mesquite could not be made for this reach):

Riparian vegetation classes	Class area	
	In hectares	In acres
Riparian wood	20	50
Mesquite	20	50
Sacaton	10	20
Unclassified <sup>a</sup>	550	1360

<sup>a</sup> This is the area outside the TMS coverage but falls within the riparian corridor from the US/Mexico border to Palominas. It does not include riparian woodland or any significant mesquite.

The figures for the total riparian corridor from the US/Mexico border to a point 3.2 km (2 miles) north of St. David are:

Riparian vegetation classes	Class area	
	In hectares	In acres
Riparian wood	640	1580
Low-density mesquite	830	2050
High-density mesquite	1490	3680
Mesquite <sup>a</sup>	20	50
Sacaton	400	980
Agriculture <sup>b</sup>	30	70
Bare soil	70	170
Scrub	2090	5160
Water	5	12
Unclassified <sup>c</sup>	550	1360

<sup>a</sup> 20 ha of mesquite from the border to Palominas (unknown density).

<sup>b</sup> This does not include fallow fields. Plowed fallow fields classified as bare soil, and old fallow fields classified as scrub. Most of the irrigated crop area falls outside of the riparian corridor.

<sup>c</sup> This is the area outside the TMS coverage but falls within the riparian corridor from the US/Mexico border to Palominas. It does not include riparian woodland or any significant mesquite.

## References

- ADWR (Arizona Department of Water Resources), 1991. Hydrographic survey report for the San Pedro River Watershed. In: The General Adjudication of the Gila River System and Source. General Assessment, Vol. 1. ADWR, Phoenix, AZ, November 20, 1991, 604 pp.
- Bowie, J.E., Kam, W., 1968. Use of water by riparian vegetation, Cottonwood Wash, Arizona. US Geological Survey Water Supply Paper 1858, 62 pp.
- Bras, R., 1990. Hydrology. Addison-Wesley, Reading, MA, p. 44.
- Brinker, R.C., 1969. Elementary Surveying, 5th Edition. Pub. International Textbook Co., Scranton, PA, pp. 33–34.
- CEC (Commission for Environmental Cooperation), 1999. Ribbon on life: an agenda for preserving transboundary migratory bird habitat on the Upper San Pedro River. CEC, Montreal, Canada, 31 pp. <http://www.cec.org>.
- Choudhury, B.J., Monteith, J.L., 1988. A four-layer model for the heat budget of homogeneous land surfaces. Quarterly J. Royal Meteorol. Soc. 114, 373–398.
- Cooper, D.I., Eichinger, W.E., Kao, J., Hipps, L., Reisner, J., Smith, S., Schaeffer, S.M., Williams, D.G., 2000. Spatial and temporal properties of water vapor and latent energy flux over a riparian canopy. Agric. For. Meteorol. 105, 161–183.
- Corell, S.W., Corkhill, F., Lovvik, D., Putman, F., 1996. A groundwater flow model of the Sierra Vista subwatershed of the Upper San Pedro Basin — southeastern Arizona. Modeling Report No. 10. Arizona Department of Water Resources, Hydrology Division, Phoenix, AZ, 107 pp.
- Croft, A.R., 1948. Water loss by stream surface evaporation and transpiration by riparian vegetation. Trans. Am. Geophys. Union 29, 235–239.
- Culler, R.C., Hanson, R.L., Myrick, R.M., Turner, R.M., Kipple, F.P., 1982. Evapotranspiration before and after clearing phreatophytes, Gila River Floodplain, Graham County, Arizona. US Geological Survey Professional Paper 655-P, 67 pp.
- Daniel, J.F., 1976. Estimating groundwater evapotranspiration from streamflow records. Water Resour. Res. 12 (3), 360–364.
- Demsey, K.A., Pearthree, P.A., 1994. Surficial and environmental geology of the Sierra Vista Area, Cochise County, Arizona. Arizona Geological Survey Open-file Report 94-6, 14 pp.
- Eichinger, W., Cooper, D., Kao, J., Chen, L.C., Hipps, L., 2000. Estimating of spatially distributed latent energy flux over complex terrain from a Raman LIDAR. Agric. For. Meteorol., 105, 145–159.
- Federer, C.A., 1973. Forest transpiration greatly speeds streamflow recession. Water Resour. Res. 9 (6), 1599–1604.
- Gatewood, J.S., Robinson, T.W., Colby, B.R., Hem, J.D., Halpenny, L.C., 1950. Use of water by bottom-land vegetation in Lower Safford Valley, Arizona. US Geological Survey Water Supply Paper 1103, 210 pp.
- Gay, L.W., Fritschen, L.J., 1979. An energy balance budget analysis of water use by saltcedar. Water Resour. Res. 15, 1589–1592.
- Goodrich, D.C., Chehbouni, A., Goff, B., MacNish, B., Maddock, T., Moran, S., Shuttleworth, W.J., Williams, D.G., Toth, J.J., Watts, C., Hipps, L.H., Cooper, D.I., Schieldge, J., Kerr, Y.H., Arias, H., Kirkland, M., Carlos, R., Kepner, W., Jones, B., Avissar, R., Begue, A., Boulet, G., Branan, B., Braud, I., Brunel, J.P., Chen, L.C., Clarke, T., Davis, M.R., Dautzat, J., DeBruin, H., Dedieu, G., Eichinger, W.E., Elguero, E., Everitt, J., Garatuza-Payan, J., Garibay, A., Gempko, V.L., Gupta, H., Harlow, C., Hartogensis, O., Helfert, M., Holifield, C., Hymer, D., Kahle, A., Keefer, T., Krishnamoorthy, S., Lhomme, J.-P., Lo Seen, D., Luquet, D., Marsett, R., Monteny, B., Ni, W., Nouvellon, Y., Pinker, R., Peters, C., Pool, D., Qi, J., Rambal, S., Rey, H., Rodriguez, J., Sano, E., Schaeffer, S.M., Schulte, M., Scott, R., Shao, X., Snyder, K.A., Sorooshian, S., Unkrich, C.L., Whitaker, M.P.L., Yucel, I., 1998. An overview of the 1997 activities of the Semi-Arid Land-Surface-Atmosphere (SALSA) Program. In: Proceedings of the Special Symposium of American Society of Meteorologists on Hydrology, Phoenix, AZ, January 11–16, pp. 1–7.
- Goodrich, D.C., Chehbouni, A., Goff, B., MacNish, B., Maddock III, T., Moran, M.S., Shuttleworth, W.J., Williams, D.G., Watts, C., Hipps, L.H., Cooper, D.I., Schieldge, J., Kerr, Y.H., Arias, H., Kirkland, M., Carlos, R., Cayrol, P., Kepner, W., Jones, B., Avissar, R., Begue, A., Bonnefond, J.-M., Boulet, G., Branan, B., Brunel, J.P., Chen, L.C., Clarke, T., Davis, M.R., DeBruin, H., Dedieu, G., Elguero, E., Eichinger, W.E., Everitt,

- J., Garatuza-Payan, J., Gempko, V.L., Gupta, H., Harlow, C., Hartogensis, O., Helfert, M., Holifield, C., Hymer, D., Kahle, A., Keefer, T., Krishnamoorthy, S., Lhomme, J.-P., Lagouarde, J.-P., Lo Seen, D., Laquet, D., Marsset, R., Monteny, B., Ni, W., Nouvellon, Y., Pinker, R.T., Peters, C., Pool, D., Qi, J., Rambal, S., Rodriguez, J., Santiago, F., Sano, E., Schaeffer, S.M., Schulte, S., Scott, R., Shao, X., Snyder, K.A., Sorooshian, S., Unkrich, C.L., Whitaker, M., Yucel, I., 2000. Preface paper to the Semi-Arid Land-Surface-Atmosphere (SALSA) Program Special Issue. *Agric. For. Meteorol.* 105, 3–19.
- Grantham, C., 1996. An assessment of the ecological impacts of groundwater overdraft on wetlands and riparian areas in the United States. EPA 813-S-96-001, 103 pp.
- Hall, F.R., 1968. Baseflow recessions — a review. *Water Resour. Res.* 4 (5), 973–983.
- Hall, R.L., Roberts, J.M., 1990. Hydrological aspects of new broadleaf plantations. In: Moffat, A.J., Jarvis, M.B. (Eds.), SEESOIL. J. Southeast England Soils Discussion Group 6, 2–38.
- Hipps, L.E., Cooper, D., Eichinger, W., Williams, D., Schaeffer, S., Snyder, K., Scott, R., Chehbouni, A., Watts, C., Hartogensis, O., Lhomme, J.-P., Monteny, B., Brunel, J.-P., Boulet, G., Schieldge, J., De Bruin, H., Shuttleworth, J., Kerr, Y., 1998. A summary of processes which are connected to evaporation of riparian and heterogeneous upland vegetation in arid regions. In: Proceedings of the Special Symposium of American Society of Meteorologists on Hydrology, Phoenix, AZ, January 11–16, pp. 13–17.
- Kingsolver, B., 2000. San Pedro River, National Geographic Society, April 2000, pp. 80–97.
- Langbein, W.B., 1942. Monthly evapotranspiration losses from natural drainage basins. *Trans. Am. Geophys. Union* 23, 604–612.
- Lines, G.C., 1996. Ground-water and surface-water relations along the Mojave River, southern California. US Geological Survey Water-resources Investigations Report 95-4189, 43 pp.
- MacNish, R., Peters, C., Schulte, M., Goodrich, D., Pool, D., Maddock III, T., Unkrich, C., Whitaker, M., Goff, B., 1998. Quantification of groundwater–surface-water interactions in a southwestern riparian system. In: Proceedings of the Special Symposium of American Society of Meteorologists on Hydrology, Phoenix, AZ, January 11–16, pp. 189–194.
- MacNish, R.D., Unkrich, C.L., Smythe, E., Goodrich, D.C., Maddock III, T., 2000. Comparison of riparian evapotranspiration estimates based on a water balance approach and sap flow measurements. *Agric. For. Meteorol.* 105, 271–279.
- Maddock III T., MacNish, R., Goodrich, D., Williams, D., Shuttleworth, J., Goff, B., Scott, R., Moran, S., Cooper, D., Hipps, L., Chehbouni, A., 1998. An overview of atmospheric and surface water coupling to regional groundwater models in semi-arid basins. In: Proceedings of the Special Symposium of American Society of Meteorologists on Hydrology, Phoenix, AZ, January 11–16, pp. 38–42.
- Magnani, F., Leonardi, S., Tognetti, R., Grace, J., Borghetti, M., 1998. Modelling the surface conductance of a broadleaf canopy: effects of partial decoupling from the atmosphere. *Plant, Cell Environ.* 21, 867–879.
- Moore, C.J., Fisch, G., 1986. Estimating heat storage in Amazonian tropical forests. *Agric. For. Meteorol.* 38, 147–169.
- Monteith, J.L., Unsworth, M.H., 1990. Principles of Environmental Physics. Edward Arnold, London.
- Moran, S., Williams, D., Goodrich, D., Chehbouni, A., Bégué, A., Boulet, G., Cooper, D., Davis, R., Dedieu, G., Eichinger, W., Everitt, J., Goff, B., Harlow, C., Helfert, M., Hipps, L., Holifield, C., Hymer, D., Kahle, A., Keefer, T., Kerr, Y., Marsset, R., Ni, W., Nouvellon, Y., Qi, J., Schaeffer, S., Schieldge, J., Scott, R., Snyder, K., Toth, J., Watts, C., Whitaker, M., Yucel, I., 1998. Overview of remote sensing of semi-arid ecosystem function in the upper San Pedro river basin, Arizona. In: Proceedings of the Special Symposium of American Society of Meteorologists on Hydrology, Phoenix, AZ, January 11–16, pp. 49–54.
- Moran, M.S., Hymer, D.C., Qi, J., Sano, E.E., 2000. Soil moisture evaluation using multi-temporal synthetic aperture radar (SAR) in semiarid rangeland. *Agric. For. Meteorol.* 105, 69–80.
- Pool, D.R., Coes, A.L., 1999. Hydrogeologic investigations of the Sierra Vista subwatershed of the Upper San Pedro Basin, Cochise County, southeast Arizona. US Geological Survey Water-resources Investigations Report 99-4197, 41 pp., 3 plates.
- Reigner, I.C., 1966. A method for estimating streamflow loss by evapotranspiration from the riparian zone. *For. Sci.* 12, 130–139.
- Richter, B.D., Richter, H.E., 1992. Development of groundwater and ecological models for protecting a southwestern riparian ecosystem. In: Stanford, J.A., Simons, J.J. (Eds.), Proceedings of the First International Conference on Groundwater Ecology. American Water Resources Association Technical Publication Series TPS-92-2. AWWA, Bethesda, MD, pp. 231–245.
- Riggs, H.C., 1953. A method for forecasting low flow of streams. *Trans. Am. Geophys. Union* 34, 427–434.
- Schaeffer, S.M., Williams, D.G., Goodrich, D.C., 2000. Transpiration of cottonwood/willow forest estimated from sap flux. *Agric. For. Meteorol.* 105, 257–270.
- Scott, R.L., Shuttleworth, W.J., Goodrich, D.C., Maddock III, T., 2000. The water use of two dominant vegetation communities in a semiarid riparian ecosystem. *Agric. For. Meteorol.* 105, 241–256.
- Shuttleworth, W.J., 1989. Micrometeorology of temperate and tropical forests. *Phil. Trans. R. Soc. London B* 324, 299–334.
- Shuttleworth, W.J., 1993. Evaporation. In: Maidment, D.R. (Ed.), Handbook of Hydrology. McGraw-Hill, New York, pp. 4.1–4.53 (Chapter 4).
- Shuttleworth, W.J., Gurney, R.J., 1990. The theoretical relationship between foliage temperature and canopy resistance in sparse crops. *Q. J. R. Meteorol. Soc.* 116, 497–519.
- Singh, K.P., 1968. Some factors affecting baseflow. *Water Resour. Res.* 4 (5), 985–999.
- Snyder, K.A., Williams, D.G., 2000. Water sources used by riparian trees varies among stream types on the San Pedro River, Arizona. *Agric. For. Meteorol.* 105, 227–240.
- Stromberg, J.C., 1998. Dynamics of Fremont cottonwood (*Populus fremontii*) and saltcedar (*Tamarix chinensis*) populations along the San Pedro River, Arizona. *J. Arid Environ.* 40, 133–155.
- Thom, A.S., 1975. Momentum, mass and heat exchange of plant communities. In: Monteith, J.L. (Ed.), Vegetation and the Atmosphere. Academic Press, New York, pp. 57–109.

- Tromble, J.M., 1983. Interception of rainfall by tarbush. *J. Range Mgmt.* 36, 525–526.
- Tschinkel, H.M., 1963. Short-term fluctuations in streamflow as related to evaporation and transpiration. *J. Geophys. Res.* 68, 6459–6469.
- Unland, H.E., Arain, A.M., Harlow, C., Houser, P.R., Garatuza-Payan, J., Scott, R., Sen, O.L., Shuttleworth, W.J., 1998. Evaporation from a riparian system in a semi-arid environment. *Hydrol. Process.* 12, 527–542.
- van Hylckama, T.E.A., 1980. Weather and evaporation studies in a saltcedar thicket, Arizona. US Geological Survey Professional Paper 491-F, 78 pp.
- Vionnet, L.B., Maddock III, T., 1992. Modeling of groundwater flow and surface water/groundwater interactions in the San Pedro River Basin: Part I — Mexican border to Fairbank, Arizona. Report HWR No. 92-010. Department of Hydrology and Water Resources, University of Arizona, 236 pp.
- Weeks, E.P., Weaver, H.L., Campbell, G.S., Tanner, B.D., 1987. Water use by saltcedar and be replacement vegetation in the Pecos River floodplain between Acme and Artesia, New Mexico. US Geological Survey Professional Paper 491-G, 33 pp.
- Whelan, D.E., 1950. A method for evaluating the hydrologic effects of land use on large watershed. *Trans. Am. Geophys. Union* 31, 253–261.
- Wolf, P.R., 1980. *Adjustment Computations*, 2nd Edition. PBL Pub. Co., Madison, WI, pp. 50–55.
- World Rivers Review, 1997. Biodiversity, North America. *World Rivers Review, News Briefs*, Volume 12, Number 1, February 1997. International Rivers Network. <http://www.irm.org/pubs/wrr/9701/briefs.html>.